Drought Characterization using Various Potential and Actual Evapotranspiration Methods

Thesis submitted in partial
fulfillment of the requirements for
the degree of

Master of Science

in

Building Science and Engineering

by Research

by

Vannam Sharath Chandra

20161157

sharathchandra.v@research.iiit.ac.in

International Institute of Information Technology,

Hyderabad (Deemed to be University)

Hyderabad - 500 032,
INDIA

April 2023

International Institute of Information Technology

Hyderabad, India

CERTIFICATE

It is certified that the work contained in this thesis, titled "Drought Characterization using Various Potential and Actual Evapotranspiration Methods" by Vannam Sharath Chandra, has been carried out under my supervision and is not submitted elsewhere for a degree.

Date: 08/05/2023

Dr. Rehana Shaik

Assistant Professor

Lab for Spatial Informatics

International Institute of Information Technology

Hyderabad, India

To My Parents Vannam Veeranna and Vasudha

Acknowledgments

I would like to take this opportunity to thank my research advisor, Dr. Shaik Rehana, without whose vision this work would not have taken form. I am grateful to Dr. Rehana for never doubting my ability to do things in different research areas and for helping me pursue the right problem statements I was passionate about working on. I thank her for being constantly supportive in the roughest times over the past few years and for motivating me to work hard through paper submissions and meet conference deadlines.

I thank my seniors, friends, Adeeba Ayaz, Pallavi Kumari, and Avantika Latwal for providing valuable inputs and domain knowledge. I appreciate the institute, IIIT- Hyderabad, for giving exposure to different research domains and the Lab for Spatial Informatics for focusing on real-world problems like water quality impacts, global environmental change, drought analysis, and remote sensing impacting society.

I especially thank my friends Raghava Muppidi, Priya Chandi, and Santhosh Vishal for patiently bearing me and helping me through some of my lowest moments. I also thank them for being curious about my work and providing insights. I also thank Avinash Nunna, Kaushik komalapalli, Annu Vishal, Shreya komal, Aashish dondeti, and Vinay Kumar for their constant support in my life.

Above everyone else, I thank my father, Mr. Vannam Veeranna, and my mother Mrs. Vasudha Vannam for inspiring and always believing in me and never giving up on me, and my sister Sharanya Gajula for caring and providing me with all the love and comfort. I thank my family members for their faith, for celebrating my every achievement as their own, and for their emotional support.

Abstract

Drought is a natural hazard with a significant impact on the economy, agriculture, and environment. It is defined as a significant decrease in water availability in all its forms. Droughts are estimated using drought indices. Drought indices are numerical measurements that describe the severity of drought by combining data from one or more variables (indicators), such as precipitation and evapotranspiration (ET), into a single number. Standardized Precipitation Evapotranspiration Index (SPEI) and Standardized precipitation Actual Evapotranspiration Index (SPAEI) are the drought indices used to estimate drought index, which take both precipitation, potential and actual evapotranspiration into account. Since ET is a critical factor in estimating drought, well-grounded ET estimations are required. The major forms of ET are Potential evapotranspiration (PET) and Actual evapotranspiration (AET). PET is described as the loss of water from a significant area that is equally covered with short, green crops that are actively growing. PET is regarded as the maximum amount of evapotranspiration. AET is defined as the total amount of water used in evaporation and transpiration by a crop during the entire growing season. Various methods have been developed to estimate PET and AET depending upon the availability of hydro meteorological variables. Various empirical based methods and hydrological model based simulations of PET and AET have been developed. Advancement of data-driven algorithms also have been extensively developed to estimate ET. In this context, many studies used empirical based estimates of ET for the calculation of drought indices. None of these studies analyzed the sensitivity of various ET methods to assess the drought characteristics. Thus, the present study aimed to include various PET and AET methods in the drought characterization. Various empirical methods, such as Penman-Monteith, Hargreaves, Turc, and Priestley-Taylor and data-driven method of Artificial Neural Network (ANN) has been used to estimate PET. The input variables used to estimate these methods are temperature, wind speed, solar radiation, and relative humidity which are obtained over the period of 1965 to 2015 for Hyderabad station. ANN model was trained and tested with climate variables as input variables and various empirical models as reference models to predict the best PET method. Penman-Monteith, Hargreaves, and Turc method performed better with ANN model estimates. Later, to study the impact of various empirical based PET estimates on drought estimation, SPEI is calculated using various PET estimates at different time scales. All other methods are compared with the Penman-Monteith method, which is considered the standard method because it considers the main meteorological factors. Hargreaves and Turc methods performed better with

the standard method and these methods can be useful in estimating drought when minimum data is available.

To assess the drought events accurately by various drought indices it is necessary to predict the hydro-meteorological variables (PET and AET) precisely. There are several challenges in estimating AET and PET at the fine spatial resolution. There are various empirical models (Budyko, Penman-Monteith, Hargreaves, and Turc) for estimating AET and PET. Still, these empirical methods does not account for the catchment characteristics, which may underestimates the actual amount of hydrological variables. Further, satellite-based remote sensing data are accessible for extracting evapotranspiration (ET) values. It provides global coverage and continuous observations of land surface variables affecting ET. Another conceptual based approach to estimate PET and AET at catchment scale is hydrological model such as Soil and Water Assessment Tool (SWAT). The present study aimed to include various approaches of empirical (Budyko, Penman-Monteith, Hargreaves, and Turc), modeled (SWAT), and remote sensing in the drought characterization using SPEI and SPAEI. Remote sensing PET and AET are considered as standard methods to compare both empirical and modeled PET and AET estimates. The present methodology was tested on a dry-sub-humid river catchment of India, the Tungabhadra River catchment. It is recommended to use PET instead of AET when estimating drought indices as SPEI values performed relatively better than SPAEI. In the present study it is observed that although PET and AET estimates vary with different models, drought indices SPEI and SPAEI are not differing much at annual scales. Hargreaves and Penman-Monteith performed better results compared to remote sensing method in SPEI calculations. And for SPAEI, Budyko and Turc performed better results. Thus, the present study concludes that empirical models correlated better with the remote sensing data. The study will be prominent for ungauged river basins, where detailed hydrological data is limited and difficult to implement hydrological models, empirical based PET and AET estimates can be better choice for drought characterization.

Content

List of Figures

List of Tables

List of Symbols

Rn	Net radiation
G	Soil heat flux
U2	Wind speed measured at 2 m height
Δ	Slope vapor pressure
g	Psychrometric constant
Ra	Extra-terrestrial radiation
α	Calibration constant
L	Latent heat of vaporization
ET	Evapotranspiration
ET_o	Reference evapotranspiration
PET	Potential evapotranspiration
AET	Actual evapotranspiration
SPEI	Standardized Precipitation Evapotranspiration Index
SPAEI	Standardized Precipitation Actual Evapotranspiration Index
PDSI	Palmer Drought Severity Index
SPI	Standardized Precipitation Index
SWAT	Soil and Water Assessment Tool
ANN	Artificial Neural Networks
SVR	Support Vector Regression
GBR	Gradient Boosting Regression
RF	Random Forest
LSTM	Long Short Term Memory
MODIS	Moderate Resolution Imaging Spectroradiometer
DEM	Digital Elevation Map
LULC	Land use Land Cover
RMSE	Root mean square error
MAE	Mean absolute error
NSE	Nash-Sutcliffe efficiency
D	Duration of the drought
S	Drought severity

Chapter 1

Introduction

1.1 Background

A drought is a period of time during which a region or area receives less precipitation than usual. Lack of sufficient precipitation, whether rain or snow, can result in lessened stream flow, crop damage, decreased soil moisture or groundwater, as well as general water scarcity. Droughts and floods are two of the most frequent and unavoidable natural calamities that affect people [1]. All life needs access to safe drinking water, and during a drought, water supplies may become scarce. Further, crops require water in order to grow and must be irrigated when not enough precipitation falls to naturally water them. During a drought period, making it impossible to irrigate crops, which leads to their demise. Precipitation and Evapotranspiration (ET) are crucial parameters to take into account when assessing drought due to their close relationship with available water resources in the hydrologic cycle [2]. Since ET is a critical factor in estimating drought, well-grounded accurate ET estimations are required. ET is when water starting from an expansive scope of sources is moved from the soil and vegetation layer to the atmosphere. Water loss from a vegetative surface through the consolidated cycles of plant transpiration, soil, and atmospheric evaporation. ET from the land surface is critical for maintaining the balance of land surface water-lakes-reservoirs as well as the energy balance of the earth surface. Since ancient times, people have understood the significance of ET in maintaining the hydrologic cycle on a continental and global scale and replenishing freshwater supplies. Water is lost from the soil surface through evaporation and from the crop by transpiration. These two processes are combined to form evapotranspiration. When liquid water is transformed into water vapor and evacuated from a surface into the air, such as a lake, soil, or moist plants, evaporation takes place. It causes heat loss from the evaporating surface in the form of latent heat, which can be compensated for by radiative or sensible-heat transfer or heat transfer from within the evaporating body to the surface. Temperature, wind speed, surface area, and humidity are the four factors that affect evaporation. Transpiration is the process through which water from plant tissues is lost to the atmosphere, mostly through a tiny hole called a stomata found in the leaves of plants and grasses. Water is absorbed from the soil through the roots and transported to the leaves via the vascular system of the roots, stem, and branches. The water is then transferred from the leaf's vascular system to the stomatal walls, where it evaporates. Like direct evaporation, the energy source, vapor pressure gradient, and wind influence transpiration. Therefore, radiation, air temperature, humidity, and wind should be considered when evaluating transpiration. The transpiration rate is also influenced by the soil water content, capacity to transport water to the roots, waterlogging, and soil water salinity. Evaporation and transpiration coincide, and it is difficult to distinguish between them. The amount of solar radiation that reaches the soil surface and the amount of water in the topsoil is the main factor affecting how quickly a cropped soil evaporates. Over the course of the growing season, this fraction falls as the crop matures and the crop canopy shades a more significant portion of the land. When the crop is tiny, soil evaporation accounts for most water loss. However, after the crop matures and has completely covered the soil, transpiration takes over as the primary mechanism.

In order to allocate water effectively, regulate irrigation, analyses the impacts of shifting land use on water output, evaluate the environment, and create optimal management practices to safeguard surface and groundwater quantity and quality, accurate measurement of ET is essential.

1.2 Motivation

Droughts are one of the most weather-related natural disasters, affecting socioeconomic and environmental systems in all temperature zones with varying frequency, severity, and duration [3] [4]. A variety of hydro meteorological processes can lead to droughts by suppressing precipitation and/or limiting surface water or groundwater availability, which can lead to conditions that are significantly drier than usual or that otherwise restrict moisture availability to a point where it could cause damage. Majorly droughts are classified into: meteorological, agricultural, hydrological, and socioeconomic [5], [6]. Meteorological drought is mostly a short-term drought occurrence that is brought on by a deficit from a lack of rainfall [7]. Rainfall deficit impact the streamflow availabilities and consequently leading to Hydrological drought [8]. It often impacts water levels from average to low, rendering them insufficient to satisfy the needs of humans and ecosystems [9]. The evaluation of hydrological drought is crucial to managing water supplies. Because human activities depend on either surface water or groundwater resources, hydrological drought assessment is critical [10]. Agricultural drought is indicated by the health of the plants and the pattern of quantitative changes in the soil moisture [11].

Drought indices serve as both indicators and tool for assessing droughts and their severity. [12], [13]. There are many different drought indicators that may be used as tools to monitor meteorological and hydrological droughts, yet there is no standard technique to describe drought conditions. Depending on the drought index in question, different input variables are needed for the computation, but they often include things like precipitation, temperature, the soil ability to store water, and other things that are indicative of the moisture in the system. The Palmer Drought Severity Index (PDSI), Palmer Z-Index, Standardized Precipitation Index (SPI), and Standardized Precipitation Evapotranspiration Index (SPEI) are a few examples of meteorological drought indexes. The goal of hydrological drought indicators is to provide a thorough description of the hydrologic effects of delayed drought. Each of these indices formulae calls for a distinct set of input variables. The most significant and well-known indicators of hydrological drought are Reclamation Drought Index (RDI), Standardized Runoff Index (SRI). Out of all drought indices, SPEI is used to estimate meteorological drought using both precipitation and PET. The climatic water balance is computed using Potential evapotranspiration (PET). Although it has been demonstrated that a variety of meteorological factors may be employed to provide accurate PET calculations, an estimation of the overall water balance is sufficient when referring to drought indices. Estimating the water balance provides additional data needed for determining Actual evapotranspiration (AET) as well as aids in keeping computations concise. [14] Originally suggested the SPEI as an enhanced drought index that is particularly suitable for research of the impact of global warming on drought severity. Similar steps are used to calculate the SPI and the SPEI. The SPEI, on the other hand, utilizes climatic water balance, which is the difference between precipitation and PET. Standardized Precipitation Actual Evapotranspiration Index (SPAEI) is similar to SPEI, with the difference being the use of AET in the place of PET. Many studies have used either empirical or hydrological, or remote sensing evapotranspiration data for drought assessment. The primary motivation of the study is to address the uncertainty due to evapotranspiration in estimating drought. The study motivated to estimate PET and AET using different methods which include empirical, hydrological, and remote sensing and calculate SPEI and SPAEI accordingly as there a necessity to study the sensitivity of PET and AET in drought assessment. The study compared empirical and hydrological based PET and AET induced drought indices to remote sensing drought index as a dependable and effective method.

1.3 Introduction

Drought indices depending on PET and AET require better estimates of these complex hydrological variables. Measurements of evapotranspiration, which combines transpiration and evaporation, can help to better understand agricultural water needs, irrigation schedules, and watershed management. There are three types of evapotranspiration: reference evapotranspiration (ET_o), AET, and PET. When water is not a limiting constraint, PET is described as the loss of water from a significant area that is equally covered with short, green crops that are actively growing. It is regarded as the maximum amount of evapotranspiration a crop may get in a specific period of time. Under the same climatic circumstances, PET cannot be greater than evaporation of surface of free water. This is true in humid environments. The evaporative power of the air, which is affected by temperature, humidity, wind, and radiation, determines the rate of PET. ET_o is a resultant of a standard calculation of the quantity of water transpired by a reference crop, usually grass, and evaporated from adjacent soil surfaces. Although both PET and ET_o provide estimates of atmospheric evaporative demand, they are based on different ideas, concepts, and application fields. They have various equations that can help to differentiate the terms. However, many researchers have treated PET and ET_o as identical concepts and used similar equations for their estimation. AET is defined as the total amount of water used in evaporation and transpiration by a crop during the entire growing season. AET remains less than maximum evapotranspiration when the available soil moisture is limited. If sufficient water is available to the crop, then the AET becomes equal to maximum evapotranspiration.

SPEI fulfills the requirements of a drought index since it is a multi-scalar character used to detect, monitor, and analyze droughts. The SPEI can evaluate drought severity based on its intensity and length and the beginning and end of drought events, just like the sc-PDSI [15] and the SPI [16]. The SPEI may be computed throughout various climates, allowing a comparison of drought severity over time and place. In addition, [17] pointed out that drought indices must be straightforward to construct, statistically reliable, and have an easy-to-understand computation process. The SPEI complies with every one of these demands. SPEI is based on the monthly difference between precipitation and PET. This is an example of a straightforward climatic water balance that is used to compute the SPEI at various time frames. However, a significant benefit of the SPEI over the most popular drought indices considering ET impact on drought severity into account is that it can identify various drought types and their effects in relation to global warming because of its multi-scalar properties. The advantages of SPEI over other indices are that they compute climatological anomalies for periods of precise duration, do not need any assumptions about the system being modelled, and simply require climatological information, which is frequently accessible and of sufficient quality. Similar to SPEI, a recent drought index of SPAEI is also assessed based on precipitation and AET. The SPAEI drought index proposal takes into account the combined impact of the meteorological and actual water budget and has the capacity to assess the consequences of climatic and hydrological changes.[18]. There are many methods to estimate PET and AET. However, the choice of PET and AET methods for drought assessment remains challenging. The uncertainty in the estimation of PET and AET can lead to any variation in the drought indicators. Hence, the study aimed to analyze drought using different PET and AET methods.

1.4 Problem definition

SPEI and SPAEI are the drought indices used to estimate drought index, which take both precipitation and evapotranspiration into account. Most studies estimated the drought index using either empirical based evapotranspiration estimates. The present study aimed to estimate the drought index of SPEI using Empirical, hydrological, and remote sensing based PET and AET estimates. PET is estimated using Empirical methods like Penman-Monteith, Hargreaves, Priestley-Taylor, and Turc. AET is calculated using empirical methods like Budyko and Turc. The hydrological method SWAT estimates both PET and AET based on the climate data estimates. Machine Learning based estimates of PET and AET were simulated using Artificial Neural Networks (ANN). Remote sensing based PET and AET estimates of Moderate Resolution Imaging Spectroradiometer (MODIS) were used to compare various empirical, modelled (hydrological). Overall, the study aimed to simulate the complex PET and AET processes using empirical (Penman-Monteith, Hargreaves, Priestley-Taylor, Budyko and Turc), data-driven (ANN) and hydrological model (SWAT). Further, the thesis aimed to study the uncertainty in the drought characterization of SPEI and SPAEI using various PET and AET estimates implemented on Hyderabad and Tunga-Bhadra River basin, India.

1.5 Thesis Organization

- Chapter 1 presents an introduction to evapotranspiration model estimates and drought indices. Problem definition, motivation, and objectives.
- Chapter 2 presents detailed literature on various PET, AET methods, and drought indices methods.
- Chapter 3 presents an introduction to the case study and datasets used.
- Chapter 4 presents the estimation of the drought index using different potential evapotranspiration models at Hyderabad station using SPEI.
- Chapter 5 presents a detailed drought analysis at the Tunga-Bhadra catchment using different PET/AET methods.
- Chapter 6 presents a summary of the thesis work, conclusions, and possible future research extensions.

Chapter 2

Literature Review

2.1 Introduction

Drought is a natural hazard with a significant impact on the economy, agriculture, and environment. It is defined as a significant decrease in water availability in all its forms. Rainfall deficits over a given period can lead to varying degrees of drought. It is one of the biggest threats to human survival. It can be distinguished in intensity, location, duration, and time. It can be considered a multilevel phenomenon guided by the response time of the basin. It should be noted that hydrological responses to soil moisture, river discharge, and groundwater discharge vary and have different response times. Therefore, the time when water deficits accumulate is crucial to determine the prevailing type of drought. Drought is simply when the soil is arid because of the amount of rainfall. When rainfall is significantly below average for an extended period of time, a drought ensues. It is a situation where there is a lack of either surface water or groundwater. Years, months, or even days may pass between droughts. A lack of water, hot, dry winds, an increase in temperature, and the subsequent evaporation of groundwater bring on drought conditions. Crop failure is a side effect of droughts as well. Droughts significantly impact the nature and agriculture of the afflicted areas. Droughts also hurt the local economy in the area. Due to the disruption to our entire ecosystem, droughts are regarded as a natural calamity. In most places of the world, drought is thought to be a regular occurrence of the climate. Because of climatic change, common droughts nowadays are more extreme and unpredictable. Drought can worsen in extremely hot climates, which eventually causes the liquid in the soil to evaporate. Any area that is hot and dry is not necessarily experiencing a drought. Drought occurrence is considerably exacerbated by the dry season. Its defining characteristics are low humidity, watering holes and cracks, and drying rivers. Land and water temperature cause droughts. More water evaporates as the temperature rises, and severe weather conditions also rise. The overall water demand steadily rises as a result of landscapes and crops needing more water to survive and develop. Drought indices are numerical measurements that describe the severity of drought by combining data from one or more variables (indicators), such as precipitation and evapotranspiration, into a single number. Compared to raw indicator data, such an index is easier to use. The form of drought indices reflects a variety of occurrences and circumstances. They can indicate abnormalities in climate dryness (mostly based on precipitation) or correspond to postponed repercussions on agriculture and hydrology, such as soil moisture loss or decreased reservoir levels. Drought indices have evolved as the main approach for informing relevant parties about the severity of the drought using this rather straightforward methodology. Weekly grid-based drought situation maps are now published and made available to the public using a few well-known indexes. Since a drought index may theoretically be developed based on a variety of variables. There are several drought indicators that have been created (more than 150, [19]).This is in addition to ongoing technological advancement (particularly in the field of remote-sensing), the requirement to tailor indices to particular climatic and hydrologic regimes (e.g., [14]), and the recent trend of combining existing indices with new ones to cover more impacts and applications (e.g.,[20]). There are several methods for characterizing droughts; nevertheless, the use of drought indicators is common [21]. Drought indices are created by adding many drought indicators to get a single numerical number. In comparison to raw data from indicators, a drought index offers a holistic picture for drought analysis and decision-making that is more easily usable [22], the performance of drought indices varies by application and specific region. Because of the complex definition of droughts, and the lack of soil moisture observations, several indices have been developed to characterize (meteorological, soil moisture, and hydrological) drought. Some examples of meteorological drought indices are the Palmer Drought Severity Index (PDSI), Palmer Z-Index, the Standardized Precipitation Index (SPI), the SPEI, and the Effective Drought Index. Out of all drought indices, the SPEI is the most commonly used drought index as it is simple and uses only precipitation and PET data, allowing for a complete approach to explore the effects of climate change on drought conditions. [14] Developed SPEI, which is sensitive to long-term trends in temperature change. If such trends are absent, SPEI performs similarly to SPI. The SPEI is calculated based on the probability that the differences between precipitation and PET are not exceeded and adjusted using a three-parameter Log-logistic. The SPEI can be estimated on various time scales to adapt to the typical drought reaction timeframes of the target natural and economic systems, allowing determination of their drought resilience. The SPEI consideration of the function of temperature through its impact on PET is a significant benefit over other multiscale drought indices like the SPI. The SPEI is, therefore, suitable for determining how droughts are affected by global warming. However, the PET-based drought indices are unable to take into account changes in land and vegetation as well as the real atmospheric water demand [23]. The transfer of moisture from the land surface to the atmosphere in response to both energy demand and moisture supply is known as AET [24]. As a result, including AET in the drought calculation can account for the actual water availability or remaining quantity of water accessible in addition to precipitation [25]. The use of AET in the formulation of SPEI has been tried by few researchers [23], [26], [27].

SPEI and SPAEI are the advanced drought indices used to estimate drought based on precipitation, PET and AET [14]. Most of the earlier studies used only empirical based PET and AET estimates in the literature. However, PET and AET estimates can be from data-driven, modeled and remote sensing. The sensitivity of PET and AET estimates can impact the drought characterization. Therefore, the present study emphasized on addressing the uncertainty of various PET and AET estimates in the drought characterization.

2.2 Estimation of Potential and Actual Evapotranspiration

Numerous attempts have been made to simulate evapotranspiration due to its significance in the water cycle, hydrological management, as well as the expensive and delicate nature of monitoring equipment. PET, AET, and reference evapotranspiration (ET_o) are significant types of evapotranspiration. PET is the amount of water lost from the surface to the atmosphere if the soil/vegetation mass has an infinite water supply. PET is the sum of soil evaporation and plant transpiration. It only happens at the potential rate when the amount of water available for this process is unlimited. AET is the rate at which water is removed from a surface to the atmosphere due to the evapotranspiration process. It is a significant component of the water balance and is utilized generally in fields such as agronomy, hydrology, climatology, meteorology, ecology, and environmental sciences. [28]–[31]. Because there is typically little water available for evapotranspiration and the exact rate of water loss is relevant, AET is the preferred form of Evapotranspiration in hydrological studies. The reference crop evapotranspiration, also known as reference evapotranspiration, is the rate of evapotranspiration from a reference surface that is not short of water. The hypothetical grass reference crop used as the reference surface has a set of features. Due to the ambiguities in other religions definitions, such as possible ET, its usage is severely forbidden. Although both PET and ET_0 provide estimates of atmospheric evaporative demand, they are based on different ideas, concepts, and application fields. They have different equations that can help to differentiate the terms. However, many researchers have treated PET and ET_0 as identical concepts and used similar equations for their estimation [32]–[35]

The estimation of PET is essential due to water constraints, population growth, and the resulting inflated food supply. This created a responsibility for the accuracy of the demand for agricultural water needs. Nevertheless, PET has been used to model and simulate structural water bodies, the hydrologic cycle, and ecosystem equilibrium. PET depends on vegetation-specific characteristics rather than solely meteorological variables; there was a need for a reference surface independent of vegetation and soil characteristics. Researchers frequently select the reference surface (grass) based on the availability of pertinent data. The grass is similar to many crops in bulk stomatal resistance and exchange values; however, shorter, trimmed grass has more experimental data. The FAO decided to utilize grass as the principal worldwide reference surface. The best model to utilize as the default model for computing PET was also discussed. To estimate PET, [36] proposed these models FAO-24 Blaney-Criddle, FAO-24 Penman, FAO-24 Radiation, and FAO-24 Pan Evaporation methodologies. The Penman-Monteith model was first proposed by Smith as the standard model for computing PET. This proposal was made based on the models past performance and the inclusion of plant physiological and aerodynamic micrometeorological parameters. The Penman-Monteith equation was formally approved as the FAO-recommended model with its release in 1998. Due to its physical foundation, it can be applied without local calibrations across various environments and climate scenarios. Second, the technique is well known and has been verified with lysimeters in various climatic settings. This equations fundamental flaw is that it calls for data on numerous climate factors unavailable in many places. The Penman-Monteith equation primary drawback is its dependence on many meteorological inputs. Apart from the Penman-Monteith equation, PET is also estimated using three other empirical methods. They are Hargreaves [37], Turc [38], and Priestley-Taylor [39]. These empirical models differ in terms of solar radiation, temperature, and transport properties of natural surfaces while considering the physical processes of radiation. [37] equation is an empirical approximation of the PET calculation based on maximum and minimum temperatures and extra-terrestrial radiation data. This method is a valuable balance between consistency and minimum data requirements. The Turc [38] method estimates PET based on the mean temperature and solar radiation. Priestley-Taylor equation can estimate regional monthly PET provided that the adjustment factor is adapted to different site conditions. Thus, PET is estimated using Penman-Monteith, Hargreaves, Priestley-Taylor, and Turc methods.

Empirical methods which presume that AET is constrained by the energy availability of PET during extremely wet conditions and by the water availability of precipitation under very dry conditions could provide promising solution for drought assessment [38], [40], [41]. Among these methods Budyko and Turc are widely used for the estimation of AET by several researchers. Although both approaches seem to be the most appropriate, their use depends greatly on the local characteristics in a particular place. Furthermore, it is crucial to employ the appropriate techniques for evaluating the critical elements of the hydrological cycle and creating a successful plan for managing water resources the more sensitive a location or station is to environmental stresses. The Estimation of AET is based on the water availability in terms of precipitation (P) and estimated PET by Penman-Monteith as it was adopted by the International Commission on Irrigation and Drainage (ICID) and the American Society of Civil Engineers (ASCE) as the standard procedure for PET.

As a result of recent advancements in hydrology using computer technology and new mathematical methods, data-driven modeling techniques have been developed as a new way for simulation and prediction. Given the accessibility of meteorological variables, empirical models may be the most suitable option for calculating the PET. Due to this constraint, some studies have advanced the evaluation of PET models by applying data-driven algorithms, including Artificial Intelligence (AI), machine learning models, and statistical regression techniques [42]. To create more accurate and effective models to estimate PET, a lot of research has been done. For example, Artificial Neural Network (ANN), Support Vector Regression (SVR), Gradient Boosting Regression (GBR), Random Forest (RF), and Long Short Term Memory (LSTM) were the main types of ML models employed for PET estimation [43]–[45]. ANN algorithms have been extensively used in the field of PET estimation in recent years. For the estimation of PET, Kumar [46] created ANN models and discovered that these models were more accurate in predicting PET than traditional empirical techniques. In more recent research, Ehteram [47] explored the modelling of PET using ANNs using the Levenberg Marquardt training method and concluded that ANNs may be successfully used to simulate PET from available climatic data. According to these researchers, the ANN can predict PET even better than the traditional FAO Penman-Monteith approach.

Several hydrological and remote sensing models are presently employed globally in PET and AET estimations [48], [49]. The Soil and Water Assessment Tool (SWAT) and the Moderate Resolution Imaging Spectroradiometer (MODIS) ET [50] product derived from remotely sensed data from MODIS instrument aboard the National Aeronautics and Space Administration (NASA) Aqua and Terra satellites will be assessed in this study as two of the more notable ones. SWAT is a physically based distributed hydrological model that simulates the flow of a larger river. SWAT has eight essential components: Hydrology, weather, sedimentation, soil temperature, crop development, nutrients, pesticides, and agricultural management. From sub-catchment scales to sub-continental scales, SWAT model have been in used in hydrological modelling.

The development of remote-sensing technology has inspired the expansion of satellite data operations that provide a range of meteorological characteristics at different scales. Estimates derived from satellites have the ability to provide the data required for a variety of applications, including drought monitoring, crop management, and water balance evaluation [51], [52]

The only dataset with fine spatial and temporal resolution suited for small-scale applications is MODIS-based PET and AET. Evaluation of satellite-based evapotranspiration products is much more constrained than other meteorological metrics. Many research, including those conducted in the USA, Australia, Europe, Africa, and East Asia, serve as examples of the work on estimating evapotranspiration using

MODIS [53], [54]. Thus, the present study used remote sensing PET and AET which is downloaded from the Appeears (https://appeears.earthdatacloud.nasa.gov) website.

2.3 Estimation of Drought Indices

Drought indices are calculated from assimilating drought indicators into a single numerical value. Compared to raw data from indicators, a drought index offers a holistic picture that is easier to utilize for drought analysis and decision-making [22]. Out of all drought indices, the SPEI is the most commonly used drought index as it is simple and uses only precipitation and evapotranspiration data, allowing for a complete approach to explore the effects of climate change on drought conditions. [14] developed SPEI, which is sensitive to long-term trends in temperature change. If such trends are absent, SPEI performs similarly to SPI. SPEI measures drought conditions based on the water balance. The SPEI is calculated based on the probability that the differences between precipitation and PET [2] are not exceeded and adjusted using a three-parameter Log-logistic. The SPEI can be estimated on various time scales to adapt to the typical drought reaction timeframes of the target natural and economic systems, allowing determination of their drought resilience. The SPEI consideration of the function of temperature through its impact on PET is a significant benefit over other multiscale drought indices like the SPI. The SPEI is, therefore, suitable for determining how droughts are affected by global warming. However, in water-limited areas, variations in AET are typically driven more by changes in precipitation than by changes in PET [55], which may make SPEI less applicable in these areas. Instead of PET, AET is used to compute the SPAEI. Thus, the present study used both SPEI and SPAEI to estimate the drought.

2.4 Research Gap areas

- Earlier studies used to calculate drought based on only empirical based evapotranspiration data.
- Due to the availability of many methods to estimate PET and AET, it is challenging to choose the correct method to estimate drought.
- None of the studies analyzed the sensitivity of various ET methods to assess the drought.

2.5 Objectives of the Thesis

The main goal of this research is to study the uncertainty in the drought characterization with various PET and AET estimates. Thus, the present study aimed to develop different methods to estimate PET and AET, like Empirical, Hydrological, Remote sensing, and Machine learning for Hyderabad station and Tunga-Bhadra catchment. The objectives of the present study are:

- To assess the applicability of different empirical-based PET methods such as Hargreaves, Turc, Priestley-Taylor and Penman-Monteith in comparison with the ANN estimates.
- To provide a comprehensive analysis of drought classification based on SPEI for different potential evapotranspiration models at 12, 6, and 3-month time scales for Hyderabad station.
- To estimate PET/AET at the Tunga-Bhadra catchment using empirical, Hydrological, and remote sensing methods.
- To study the uncertainty in the drought characterization with various PET, AET estimates using SPEI and SPAEI at the Tunga-Bhadra catchment.

.

Chapter 3

Study Area and Data

3.1 Introduction

The present study has selected two study areas with diverse climatological conditions. The first one is Hyderabad the largest city of the Indian state of Telangana. The second case study considered is Tunga-Bhadra Catchment.

3.2 Study area

Hyderabad:

Hyderabad, lies between latitude 17.3850°N and 78.4867°E located on the Deccan Plateau in the northern part of South India and covers an area of 650 square kilometers (250 sq. mi) in an elevation of 542m. Based on the Koppen climate classification, the climate is tropical wet and dry, bordering on a hot semi-arid, with an average annual precipitation of about 171 mm (https://en.climate-data.org/asia/india/hyderabad). To study the uncertainty of PET estimates on SPEI, the present study used Hyderabad as case study. To implement various PET methods such as Penman-Monteith method, various meteorological data (temperature, radiation, etc.) is required. Further, to implement data-driven methods to estimate PET, a long-time series data without any missing data points is required. Daily meteorological data were obtained from January 1965 through December 2015 (51 years) (612 months) from the weather station situated in Professor Jayashankar Telangana State Agricultural University, Rajendranagar Mandal, Hyderabad, Telangana. The statistical values of the meteorological variables are presented in Table 3.1. Five monthly meteorological variables were recorded, including (1) maximum air temperature (T_x °C); (2) minimum air temperature (T_n °C); (3) wind speed (U_2 ms $^{-1}$); (4) mean relative humidity (RH_{mean}%) and (5) solar radiation (Rs, MJ m^{-2} d^{-1}). Measurements were made at 2m height (air temperature and relative humidity) and 10 m (wind speed) above the soil surface. Wind speed data at 2 m (U_2) were obtained from those taken at 10 m using the log-wind profile equation.

Table 3.1: Statistical values of meteorological variables and PET at Hyderabad station

Parameters	T_x	T_n	RH_{mean}	U_2	R_s	PET
Maximum	45.5	33.0	100	189.90	14.45	13.16
Minimum	17.6	5.0	6	0	3.55	0.005
Mean	32.37	19.88	78.43	6.27	9.32	3.76
Standard Deviation	4.1	4.79	14.48	6.18	2.44	1.72

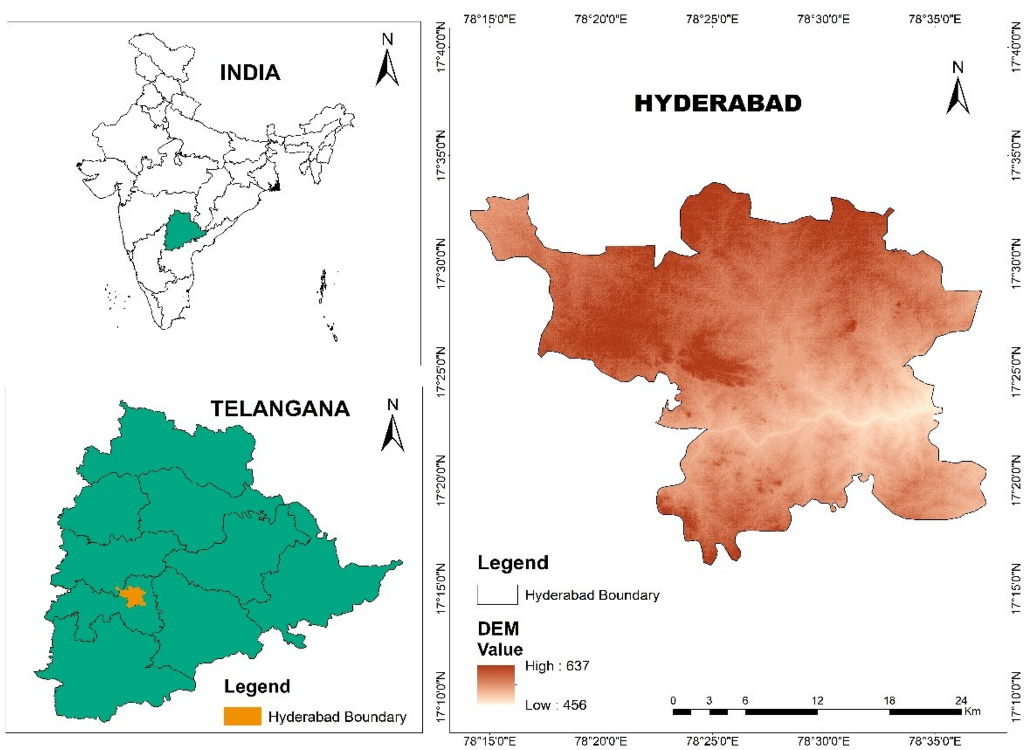

Figure 3.1: Case study: Hyderabad, Telangana, India

Tunga-Bhadra:

To study the drought analysis including various PET and AET estimates, the present study considered Tunga-Bhadra river basin, which is a major tributary of Krishna river basin, India is considered. The Tunga-Bhadra River is formed by the junction of two rivers, the 147 kilometers Tunga River and the 178 kilometers Bhadra River, rising in the Western Ghats with a confluence at Koodli, Shimoga district, Karnataka. It runs as the Tunga-Bhadra for 531 kilometers from Karnataka to Andhra Pradesh until it joins the river Krishna at Sangameshwaram near Kurnool. The catchment area considered for the present research work is the part of the Tunga-Bhadra sub-basin of the Krishna river basin that lies upstream of the Tunga-Bhadra dam and spans over 28,845 Km^2 up to the Tunga-Bhadra reservoir, which is at the outlet of the catchment. The mean sea level elevation of the Tunga-Bhadra river catchment is 641 meters, and the catchment area lies between the geographical coordinates of $13^0$10'N - $15^0$45' N and $74^0$50'E – $76^0$30'E. Tunga-Bhadra, a sub-basin of the Krishna basin, is one of the drought-prone regions of India, along with an increase in the temperature in that region [56]. Daily meteorological data (temperature, wind speed, relative humidity, and solar radiation) were obtained from 2000 to 2013 through climate forecast system analysis (CFSR) Droughts are more common in this region compared to floods. In the water resources scenario context, understanding the surface water availability and demands and the severity of the hydrologic extreme of droughts is essential [57]. The present study focused on modeling hydrologic variables in various ways for drought severity assessment.

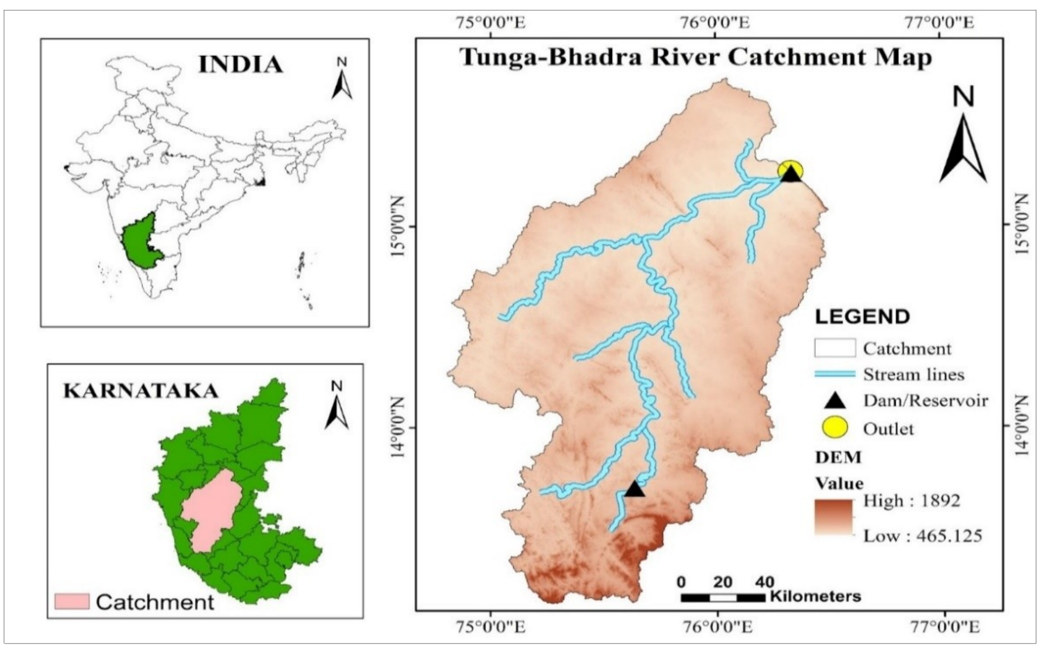

Figure 3.2: Case Study: Tunga-Bhadra catchment

The various meteorological datasets (precipitation, temperature, wind speed, relative humidity, and solar radiation), Hydrological datasets (Digital elevation model, Land use and land cover, Streamflow, and soil) used in the present study are presented in Table 3.2 and 3.3

Table 3.2: Details of the Datasets used in the study

Data Types	Year	Source
	2012	Shuttle Radar Topography Mission (SRTM)
Land Use Land Cover(LULC)	2012	SWAT2012 Datasets
Streamflow	2005 to 2013	Advanced Centre for Integrated Water Resources Management (ACIWRM)
Soil Map	2012	SWAT2012 Datasets
Precipitation	2000 to 2013	Advanced Centre for Integrated Water Resources Management (ACIWRM)
Temperature, Wind speed, Relative Humidity, Solar Radiation	2000 to 2013	Climate Forecast System Reanalysis (CFSR)
Remote Sensing PET and AET	2000 to 2013	Moderate Resolution Imaging Spectroradiometer (MODIS)

Table 3.3: Statistical values of meteorological variables and PET at Tunga-Bhadra catchment

Parameters	T_x	T_n	RH_{mean}	U_2	R_s	PET
Maximum	43.26	25.04	96.27	7.83	27.81	8.75
Minimum	18.80	7.05	19.60	0.84	1.24	0.11
Mean	30.37	18.96	67.52	2.75	17.54	2.13
Standard Deviation	5.09	2.83	19.33	0.84	6.19	1.67

3.3 Summary

The present study considered urban semi-arid region, Hyderabad as case study to find the uncertainty of PET estimates in drought assessment using SPEI as presented in chapter 4. Daily meteorological data of the Hyderabad case study from 1965 to 2015 as discussed in the present chapter has been used to estimate PET using various empirical methods of PET as presented in Chapter 4. Furthermore, to study the uncertainty of various PET and AET estimates from empirical, hydrological and remote sensing observations in the drought assessment at catchment scale, the present study considered Tunga-Bhadra river basin as case study. Climate data from 2000 to 2013 as discussed in the present chapter has been used to calculate PET and AET using different methods (Chapter 5). Both PET based drought index of SPEI and AET based drought index of SPAEI has been used to understand the drought characteristics of Tunga-Bhadra River basin as presented in Chapter 5.

Chapter 4

Estimation of Drought Index using different potential evapotranspiration models at Hyderabad, India

4.1 Introduction

In this present chapter, data-driven algorithm ANN is used to compare various empirical based PET estimates using various climate variables. Four empirical methods Penman-Monteith, Hargreaves, Turc, and Priestley-Taylor were used to estimate PET at a daily time scale. The input variables for ANN model consist of maximum and minimum air temperatures, relative humidity, solar radiation, and wind speed. ANN model was trained and tested with climate variables as input variables and various empirical models as reference models to predict the best PET method. Later, to study the impact of various empirical based PET estimates on drought estimation, the present study calculated drought using SPEI drought index using various PET estimates at different time scales. All other methods are compared with the Penman-Monteith method, which is considered the standard method because it considers the main meteorological factors. These PET models are used to understand the variation of drought in the period of consideration (1965-2015) over an urban semi-arid region, Hyderabad, the capital of the Indian state of Telangana. The accuracy of the SPEI largely depends on the selected PET method. This chapter provides a detailed description of PET methods and their impact on drought estimation.

4.2 Estimation of Potential Evapotranspiration

The PET values for the Hyderabad station are calculated using empirical methods and a data-driven model. Empirical methods include FAO Penman-Monteith, Hargreaves, Turc, and Priestly Taylor. ANN is used as a data-driven model.

4.2.1 FAO Penman-Monteith Method

The FAO Penman-Monteith method is recommended as the standard method. It is a method that has a good chance of correctly forecasting PET in various regions and climates. The variables required to calculate using this method are temperature, relative humidity, wind speed, and solar radiation. The equation is given as

$$PET = \frac{0.408\Delta(R_n - G) + g(\frac{900}{T+273})U_2(e_s - e_a)}{\Delta + g¿¿}$$

(4.1)

Where R_n is the net radiation at crop surface (MJ m^{-2} d^{-1}), G is the soil heat flux (MJ m^{-2} d^{-1}), T is the average temperature at 2 m height(°C), U_2 is wind speed measured at 2 m height [m s^{-1}], (e_s - e_a) is pressure deficit for measurement at 2 m height [k Pa], Δ is slope vapor pressure curve [k pa°C^{-1}], g is psychrometric constant [k pa°C^{-1}], 900 is Coefficient for the reference crop [l J^{-1} Kg K d^{-1}], 0.34 is wind coefficient for the reference crop [s m^{-1}]

4.2.2 Hargreaves Method

Hargreaves equation for the formulation of PET can be helpful balance between consistency and minimum data requirements. The Hargreaves method is estimated based on maximum and minimum temperatures. The equation is given as

$$PET = 0.0023 * R_a * (T_m + 17.8) * (T_d^{0.5}) \quad (4.2)$$

Where T_d is the difference between maximum temperature and minimum temperature (°C), T_m is the mean temperature (°C), and R_a is extra-terrestrial radiation (mm/d).

4.2.3 Turc Method

Turc developed an equation to simplify an older equation for calculating PET. The Turc method estimates PET based on mean temperature and solar radiation. The equation is given as

$$PET = 0.013 * (T_m + 15) * (23.88\, R_s + 50) \quad (4.3)$$

Where, Tm is the mean temperature (°C), solar radiation (Rs) is [0.25 + 0.5 (n/N)] Ra, Ra is extra-terrestrial radiation (mm⁄d), n is actual hours of bright sunshine (hrs.), N is maximum possible hours of sunshine (hrs.).

4.2.4 Priestley-Taylor Method

The Priestley-Taylor model is a condensed version of the original Penman combination equation. This method estimates PET using net radiation and latent heat of vaporization. The equation is given as

$$PET = \alpha(\frac{\Delta}{\Delta + g})(\frac{R_n - G}{L}) \quad (4.4)$$

$$\Delta = 4098¿¿ \quad (4.5)$$

Where Δ is slope vapor pressure curve psychrometric constant [k pa°C^{-1}], R_n is the net radiation at crop surface (MJ m^{-2} d^{-1}), α is a calibration constant 1.26, L is the latent heat of vaporization. It can be considered as 2.45 (MJ/kg), which is constant.

4.2.5 Artificial Neural Networks (ANN)

An artificial neural network (ANN) is an algorithm that was developed to create devices that could mimic the brain [58]. An interconnected collection of artificial neurons makes up a neural network. Biological structures can gather, store, and apply experiential knowledge. Like the human brain, the ANN learns from the instances it encounters. It learns from its experience and errors in a nonlinear parallel processing manner. ANNs are fully connected neural nets that consist of an input layer, hidden layers (multiple or single), and output layers. Each node can be considered a neuron. Each neuron is linked to at least one other neuron, and the weight coefficient measures the strength of each connection, that reflects the degree of importance of the given connection in the neural network [59] Each node takes the weighted sum of its inputs which then passes through a nonlinear activation function (like RELU, sigmoid, tanh, etc.), which then becomes the input of other nodes in the next layer. The neuron is the fundamental calculating entity that computes several inputs, delivers one output compared with a threshold value, and turns on (fired). The computational processing is done by internal structural arrangement consisting of hidden layers that utilize the backpropagation and feed-forward mechanism to deliver output close to accuracy. The error between the predicted output value and the actual value is back-propagated through the network to update the weights. This method is proven highly successful in the training of multi-layered neural networks. The logistic sigmoid transfer function is the most often utilized activation function in neural networks. This function transforms an input value into an output with a value between 0 and 1. Depending on the sign of the threshold weight, the impact of the threshold weights is to move the curve to the right or left, changing the output value from higher to lower. By computing the weighted total and including bias, the activation function determines whether a neuron should be turned on. The motive is to introduce non-linearity into the output of a neuron. In Eq 4.6, the function f represents the activation function, w is the weight matrix, and x is the input vector set. (https://medium.com/@ariesiitr/an-artificial-neural-network-ann-is-a-computational-model-that-is-inspired-by-the-way-biological-c17b07166d4c)

$$Z = f(x\,w) = f\left(\sum_{i=1}^{n} x_i w_i\right) \; x \in d_{1\times n,} \, w \in d_{n\times 1,} \, z \in d_{1\times 1,} \qquad (4.6)$$

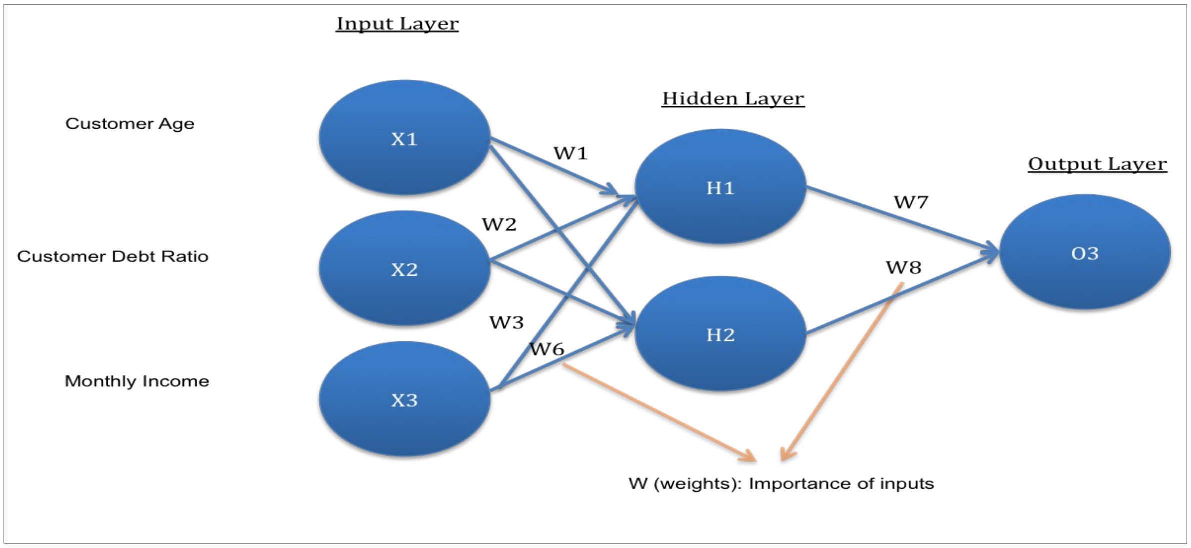

Figure 4.1: Structure of ANN used for training a model with hidden layer and weights and the output layer showing a feed-forward pass- xi wi

This study used a feed-forward backpropagation neural network. The weights are initially randomly assigned. The train: test spilt on the dataset is 7:3. A forward pass is performed for every training data using the current weights, and the output is calculated for each node. The final output is acquired at the last node, and the error is calculated with a loss function. Now, a backward pass is performed to estimate the contribution of each node in error calculated. The error is propagated to every single node using backpropagation. Once the contribution of each node has been calculated, the weights are adjusted accordingly using gradient descent. The present study used gradient descent with momentum and adaptive linear regression. The procedure is repeated until the loss function gives an error less than the threshold value, and the weights and bias of the required network are thus obtained. Thus, the model converges, and a definite result can be obtained for any testing dataset. The data from 1951-2015 were divided into two subsets of training and testing using the earlier approach. The employed approach for splitting the data ensured that the sub-datasets fairly represented the population to be modeled. The training subset optimized the networks connection weight matrices and bias vectors. Once the network was trained, the generalization and predictive ability of the network were evaluated using a completely unseen subset called the testing subset. This method did not presuppose the PET mechanisms physics or the variables interrelationships. All feasible input variable combinations, a total of 26 combinations, were considered ANN model input sets. Separate optimum ANN models were created and trained using the previously described model creation methodology. The created ANN models prediction accuracy was compared to determine the most effective and appropriate input combinations for PET estimation. This strategy sometimes referred to as a trial-and-error process, is a heuristic approach.

4.3 Estimation of Standardized precipitation evapotranspiration index (SPEI)

The standardized Precipitation Evapotranspiration Index (SPEI) takes precipitation and PET into account. The likelihood that the disparities between precipitation and PET are not exceeded is used to determine the SPEI, which is then corrected using a three-parameter Log-logistic. Precipitation is a crucial factor in determining the SPEI, which is used to assess drought conditions. Higher the precipitation can result in higher SPEI values, indicating wetter conditions. Conversely, lower precipitation can result in lower SPEI values, indicating drier conditions. However, SPEI depends on the deviations of both precipitation and potential evapotranspiration. It is estimated at different time scales. The SPEI at different time scales represents different climatic water balances. The difference between P and PET for a month *i* is given as

$$D_i = P_i - PET_i \tag{4.7}$$

For example, to obtain a 12-month SPEI time series is constructed by the sum of D values from 11 months, i.e., before to the current month.

The calculated D_i values are aggregated at different time scales, given as

$$D_n^k = \sum_{i=0}^{k=1} P_{n-1} - (PET)_{n-1} \tag{4.8}$$

Where *k* is the aggregate time measure (months), and *n* is the calculation month. The probability density function for the logistic distribution is given as

$$f(x) = \frac{\beta}{\alpha}\left(\frac{x-\gamma}{\alpha}\right)^{\beta-1}\left[1+\left(\frac{x-\gamma}{\alpha}\right)^{\beta}\right]^{-2} \tag{4.9}$$

Where α, β and γ are the scale, shape, and origin parameters, respectively, for γ> D <∞. The probability distribution function for the D series is given as follows

$$f(x) = \left[1+\left(\frac{\alpha}{x-y}\right)^{\beta}\right]^{-1} \tag{4.10}$$

With f(x), the SPEI can be obtained as the standardized values of f(x) where

$$SPEI = W - \frac{C_o + C_1 W + C_2 W^2}{1 + d_1 W + d_2 W^2 + d_3 W^3}$$

$W = \sqrt{-2\ln(P)}$ For $P \leq 0.5$

(4.11)

The constants are: C_0 = 2.515517, C_1 = 0.802853, C_2 = 0.010328, d_1 = 1.432788, d_2 = 0.189269, and d_3 = 0.001308.

Positive SPEI values indicate average humidity conditions, while negative values indicate drier conditions. A drought is defined when the SPEI value is less than or equal to -1 in a given period. The drought categories according to SPEI values are given below

Table 4.1: Drought classification based on SPEI values ***[14]***

Moisture Category	SPEI Value	Drought classification
Extremely wet	2.00 and above	No drought
Very Wet	1.50 to 1.99	No drought
Moderately wet	1.00 to 1.49	No drought
Near Normal	-0.99 to 0.99	No drought
Moderately dry	-1.00 to -1.49	Moderate Drought
Severely dry	-1.50 to -1.99	Severe Drought
Extremely dry	-2.00 and less	Extreme Drought

The original classification thresholds for drought severity categories were developed for the Standardized Precipitation index (SPI), which is a precipitation-based index. It was introduced by McKee [16]. Based on his study, there are total of seven categories for drought classification. Later SPEI was introduced by Vicente-Serrano [14]. It is an extended concept of SPI and uses the same values as classified in Table 4.1. Many research studies have used the same table for the classification of drought. [60], [61]

4.4 Evaluation metrics

The accuracy of the ANN models is validated using Root mean square error (RMSE), Mean absolute error (MAE), and Coefficient of determination (R^2).

RMSE, MAE, and R^2 are common metrics used in regression analysis to assess the performance and goodness of the fit of a model. RMSE measures the average error between predicted and actual observed values. Lower RMSE values indicate smaller errors and better accuracy of the model, with zero RMSE indicating a perfect fit.

MAE measures the average absolute difference between predicted and actual observed values. Similar to RMSE, lower MAE values indicate smaller errors and better accuracy of the model. A MAE value of zero would indicate a perfect fit.

R^2 on other hand, measures the proportion of the total variation in the dependent variable that is explained by the regression model. R^2 values ranges from 0 to 1, with 1 indicating a perfect fit

$$RMSE=\sqrt{\frac{1}{N}\sum_{i=1}^{n}\left(O_i-S_i\right)^2} \qquad (4.12)$$

$$MAE=\frac{1}{N}\sum_{i=1}^{N}\left(O_i-S_i\right) \qquad (4.13)$$

$$R^2=1-\frac{\sum_i\left(O_i-S_i\right)^2}{\sum_i\left(O_i-\acute{O}\right)^2}$$

(4.14)

Where O_i is the observed values, S_i is the simulated values, $\acute{O}$ is the mean value of O, and N is the total number of data points.

4.5 Results and Discussions

The climate variables considered for estimating daily PET using ANN and Penman-Monteith methods were the daily maximum temperature, minimum temperature, relative humidity, wind speed, and solar radiation. Similarly, the input variables considered for the Turc and corresponding ANN model are temperature and solar radiation. For the Hargreaves and corresponding ANN model, maximum temperature, minimum temperature, and solar radiation are input variables. Furthermore, for the Priestly-Taylor method, the input variables used in ANN are temperature, solar radiation, and relative humidity. All these methods uses different combinations of input variables. Since all these methods are energy based methods, these methods are compared under similar climatic and data conditions. The ANN model used in the present study is Multi-Layered Perceptron (MLP) imported from the scikit-learn library in python. The study used three hidden layers with several neurons same as the number of features or parameters, i.e., 6 (maximum air temperature, minimum temperature, maximum relative humidity, minimum relative humidity, wind speed, and solar radiation), and ran the model for 500 iterations. Convergence was obtained for the datasets of all four empirical methods.

The prediction values have been calculated by fitting the test data on the trained model. As the number of meteorological variables for each empirical method is different, therefore, for each empirical model, an ANN model was trained, and results were tested. The input vector has the features considered in each method (Penman-Monteith, Hargreaves, Turc, and Priestley-Taylor) 3 hidden layers have been used for each method, and the output vector is the expected PET networks hidden layer was determined using a trial and error method by considering the MAE, RMSE, and R^2 values from a test sample. This study trained ANNs for 500 epochs with one to 6 nodes in the hidden layer. As mentioned, statistical parameters were calculated using only the real test data set after each training run. The training period is from 1965 to 2000, and the testing is from 2001 to 2015. The validity and efficiency of the model can be seen when the training dataset is fit the trained model, and high accuracy and minimal values of RMSE were obtained. The performance of each empirical model corresponding with the ANN model in terms of R^2, RMSE, and MAE is listed in Table 4.2. From Table 4.2, it can be concluded that Penman-Monteith method correlated better with the data-driven model. Hargreaves, Turc are correlated comparatively better than Priestley-Taylor method. As shown in Figure 4.6, some deviations occurred for Priestley-Taylor method.

The PET results shown in Figure 4.2 are calculated on an annual basis. In this figure, the Priestley-Taylor method produces lower values, while Hargreaves produces higher values with a significant difference of about 1200 mm in mean values. The PET values produced by the Hargreaves method are close to the Penman-Monteith Method compared to other methods. In this study, the FAO Penman-Monteith method is considered the reference method as it requires more meteorological data to calculate. Figure 4.3 to 4.10 shows the comparison between daily PET values from empirical models of Penman-Monteith, Priestley-Taylor, Hargreaves, Turc, and ANN methodologies for training and testing datasets.

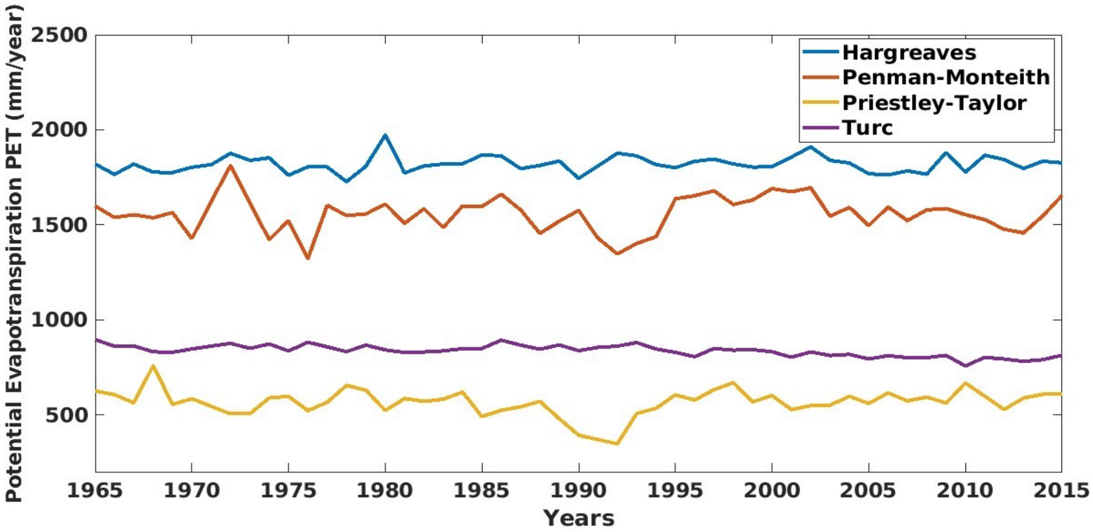

Figure 4.2: Yearly Potential evapotranspiration (PET) using Hargreaves, Penman-Monteith, Priestley-Taylor,andTurc method

Table 4.2: Statistical summary of testing and training period for ANN

Empirical Methods	Artificial Neural Network (Training)			Artificial Neural Network (Testing)		
	R^2 (0 to 1) Best is 1	RMSE (0 to ∞) Best is 0	MAE (0 to ∞) Best is 0	R^2 (0 to 1) Best is 1	RMSE (0 to ∞) Best is 0	MAE (0 to ∞) Best is 0
Penman-Monteith	0.97	0.02	0.008	0.96	0.03	0.009
Turc	0.96	0.03	0.007	0.95	0.04	0.012
Hargreaves	0.94	0.05	0.015	0.94	0.06	0.017
Priestley Taylor	0.91	0.10	0.022	0.92	0.12	0.025

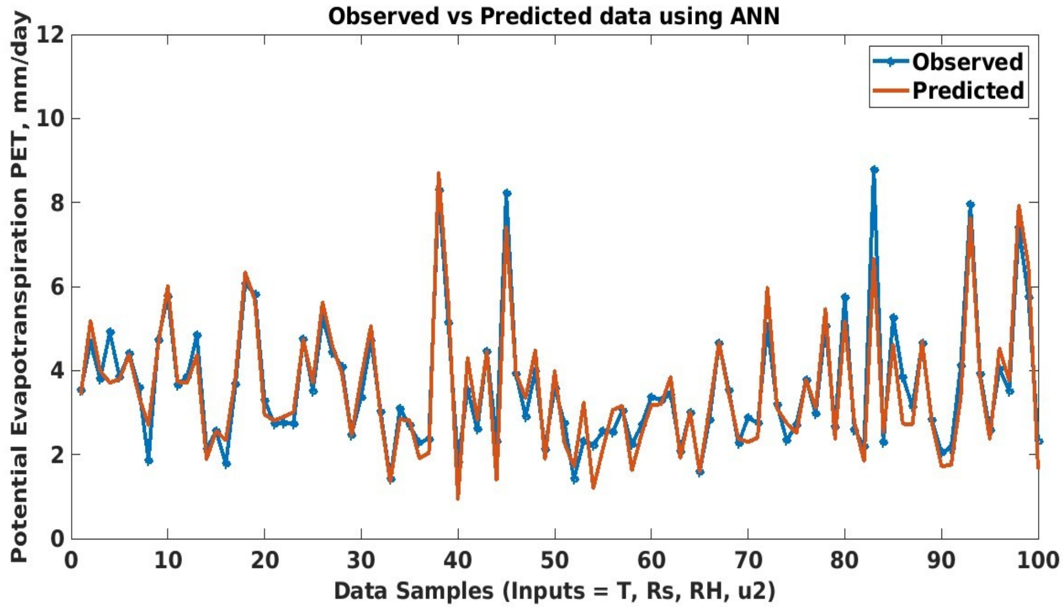

Figure 4.3: Variation in Potential evapotranspiration (PET) for Penman-Monteith method forthe first 100 data points using ANN

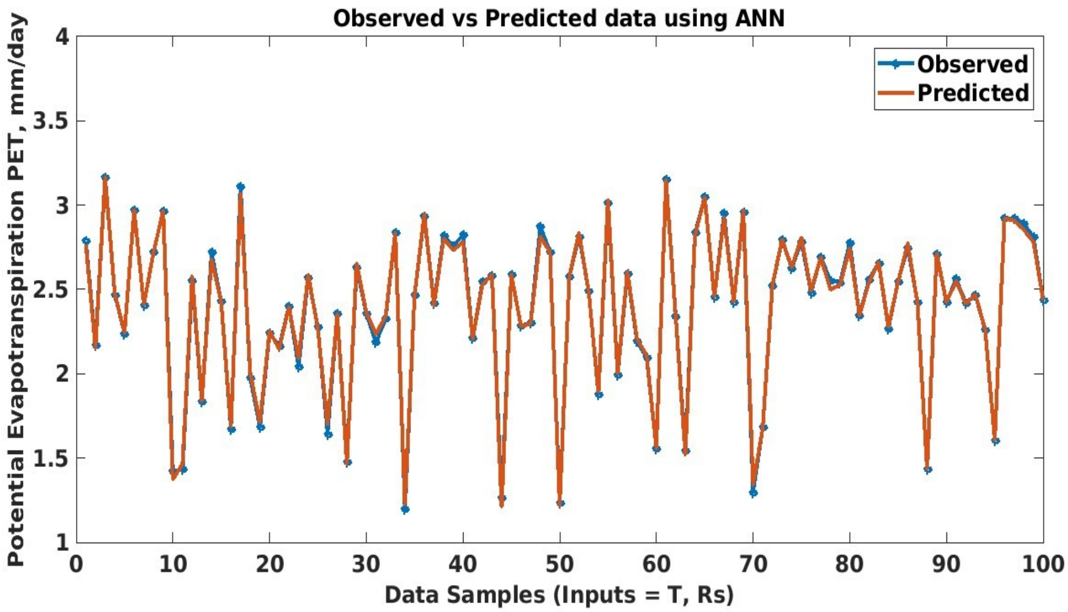

Figure 4.4: Variation in Potential evapotranspiration (PET) for Turc method for the first 100 data points using ANN

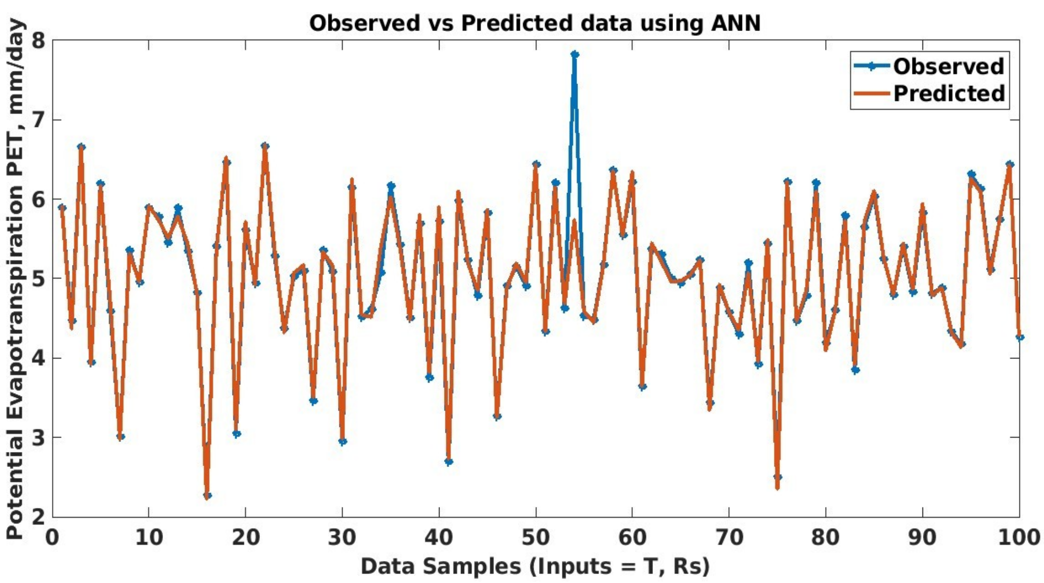

Figure 4.5: Variation in Potential evapotranspiration (PET) for Hargreaves method for The first 100data points using ANN

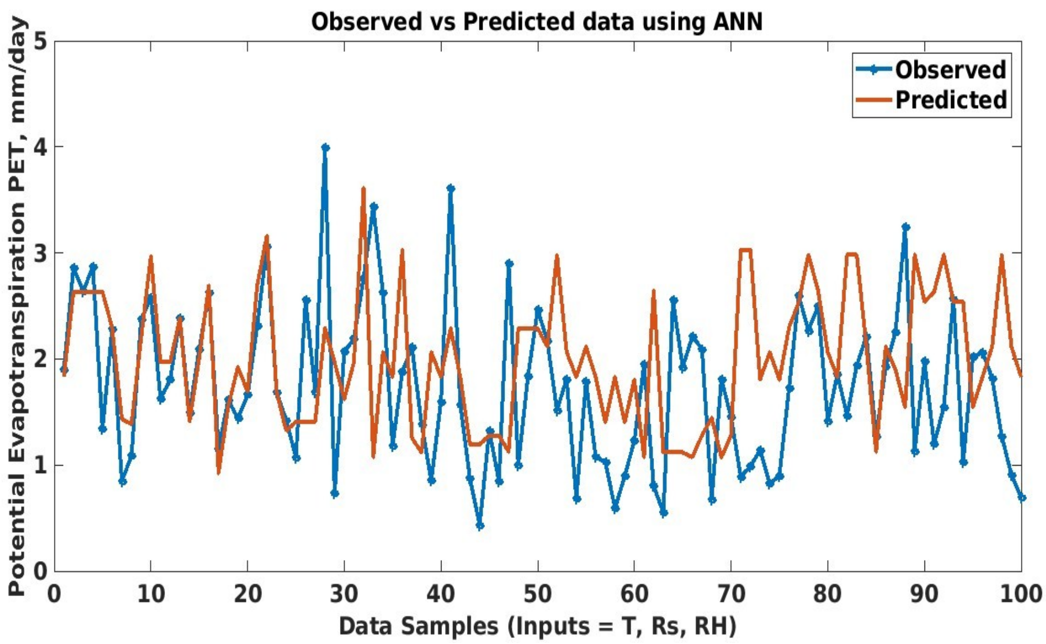

Figure 4.6: Variation in Potential evapotranspiration (PET) from Priestley – Taylor for The first 100 data points using ANN

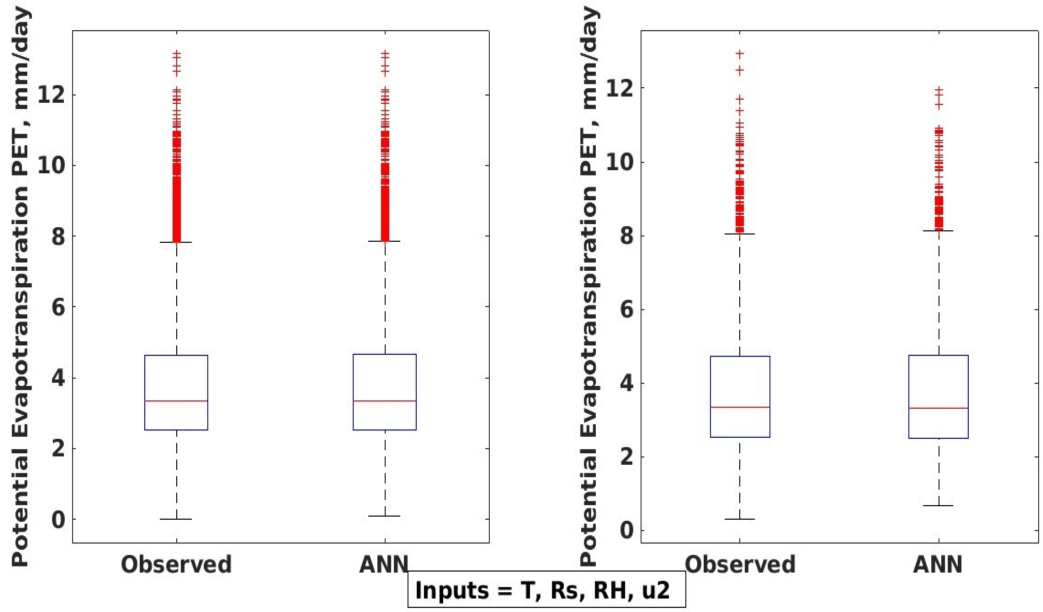

Figure 4.7: Comparison of PET predicted by ANN and Penman-Monteith method Values for training and testing periods

Figure 4.3 compares PET daily values predicted by the ANN model versus the PET values of the Penman-Monteith method for both testing and training periods. A good correlation was observed with R^2 values higher than 0.96, RMSE as 0.03, and MAE as 0.009 between the Penman-Monteith method and ANN for the testing period. The trained and tested ANN model performs very well compared to Penman-Monteith estimates. The comparison shows that neither overestimation nor underestimation was produced in the range of the values studied. This verifies that the ANN models can be used to estimate PET values. Thus, compared to all empirical models, the Penman-Monteith has been predicted well with the data-driven algorithm of ANN. It can be noted that, as the Penman-Monteith method accounts for all climate variables in modeling, such accuracies were expected to be comparable to other empirical models.

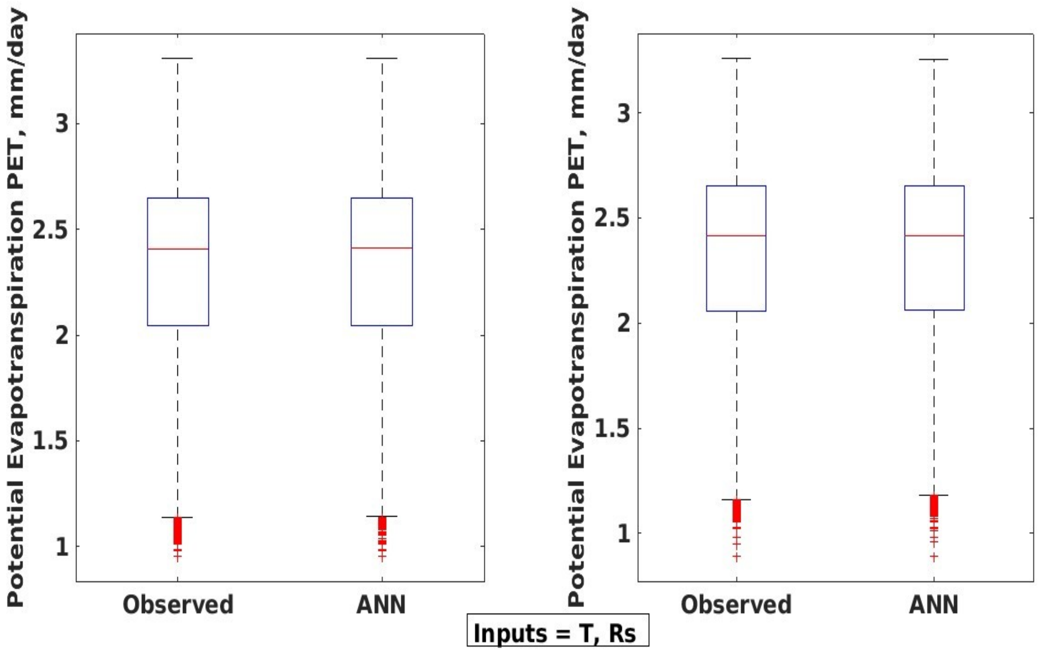

Figure 4.8*:* Comparison of PET predicted by ANN for Turc method values for training and testing periods.

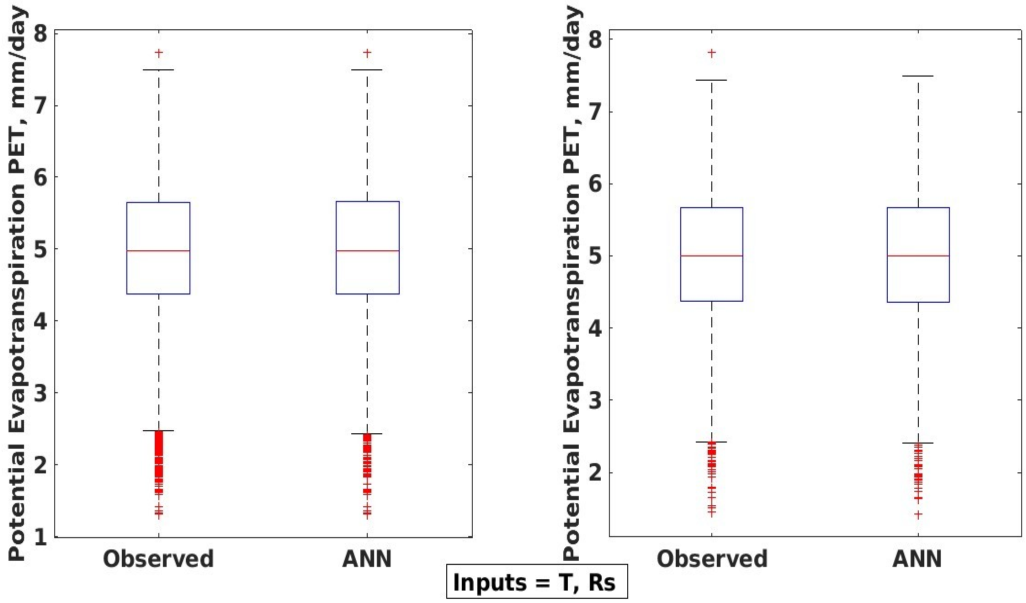

Figure 4.9: Comparison of PET predicted by ANN for Hargreaves method values for training and testing periods

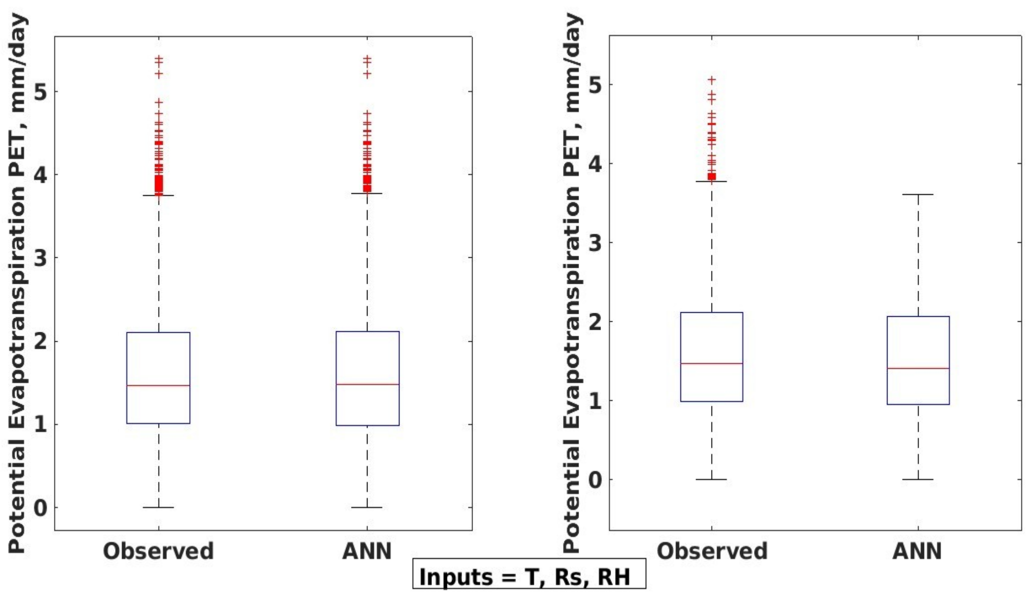

Figure 4.10: Comparison of PET predicted by ANN for Priestley – Taylor method Values for training and testing periods

Furthermore, the present study tried to understand the sensitivity and dependency of each meteorological variable on the modeled PET using the Penman-Monteith model. The study plotted the scatter plots between each climate variable and PET modeled, as shown in Figure 4.11.

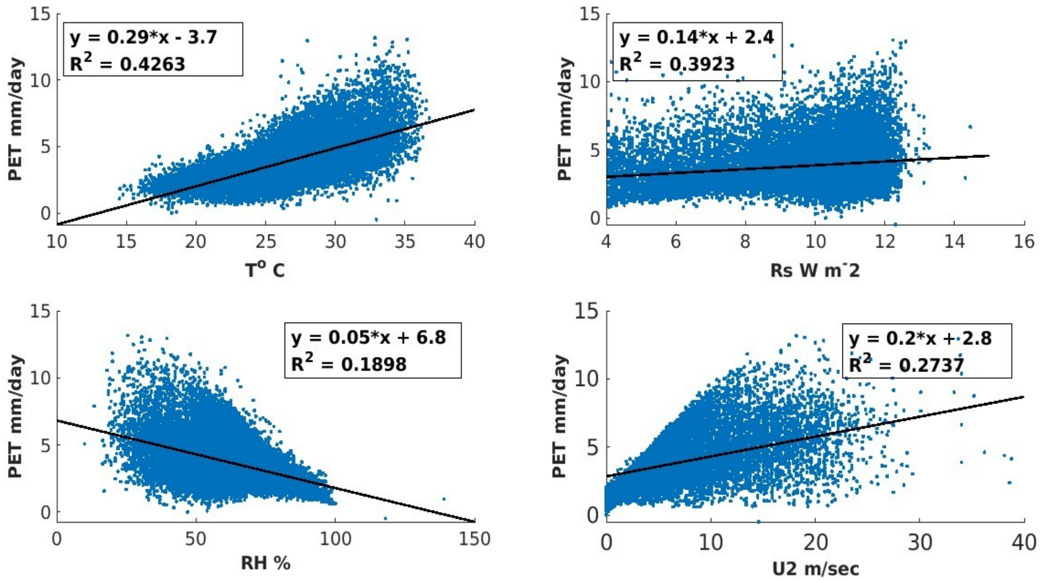

Figure 4.11: Correlation of main meteorological parameters such as temperature, relative humidity, solar radiation, and wind speed to PET

As shown in Figure 4.11, the temperature, solar radiation, and wind speed, followed by relative humidity, have the most substantial influence on PET estimations based on the Penman-Monteith model. Therefore, ANN models were derived based on temperature, solar radiation, and relative humidity as input and the PET as output variables. Furthermore, the results of the ANN can be significantly influenced by the number of input data which can lead to significant error and deviation. On the other hand, lowering the number of neurons in the input layer to three or even two can give us satisfactory results in estimating the PET. The most critical inputs for accurately estimating PET using an ANN are temperature and radiation data [62]. The findings demonstrated that selecting the right ANN design enhances the link between the dependent and independent variables while minimizing error.

The study results reveal that temperature and solar radiation are the most influencing variables compared to relative humidity and wind speed for semi-arid climate conditions, as demonstrated in the present study. Given the intense data requirements for applying the Penman-Monteith model, the study employed ANN with minimum input variables such as temperature, solar radiation, and relative humidity. The trained and tested algorithms developed based on empirical models can be valuable tools to predict PET for limited data case studies. Analyzing the sensitivity of each climate variable on PET, testing the statistical dependencies, and data pre-processing to acquire relevant information before developing such data-driven algorithms are the most important in the implementation. Analysis of compensating accuracies with the inclusion of limited climate input variables in the PET estimates compared to standard empirical models can be a potential area of research.

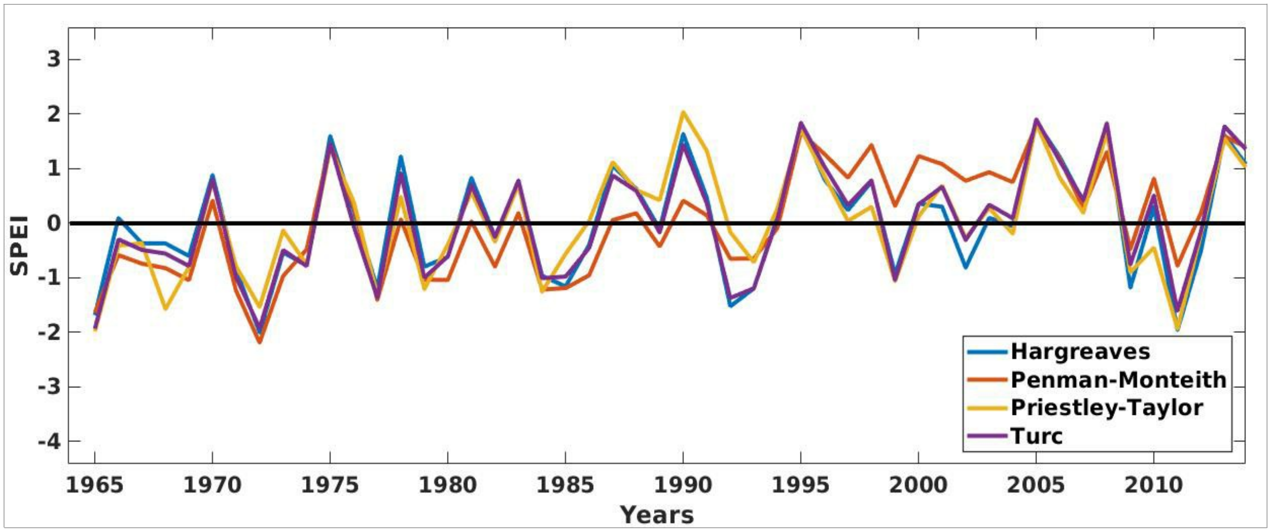

Figure 4.12: Annual SPEI calculated for the different PETmethods.

Table 4.3: Performance statistical indicators of SPEI values calculated by various PET methods against the reference method

Method	RMSE (mm)	MAE (mm)	R^2
Hargreaves	0.624	0.010	0.76
Priestley-Taylor	0.714	0.029	0.54
Turc	0.508	0.003	0.66

The next step is to calculate SPEI using various PET-based empirical estimates. The SPEI values calculated for 12 month accumulation period are shown in Figure 4.12. Table 4.1 gives the drought classification based on SPEI values. If the SPEI value is >-1, there is no drought. If SPEI is in the range of -1.0 to -1.49, it is Moderate drought; -1.5 to -1.99, it is severe drought; and -2 and less, it is Extreme drought. The comparison based on statistical performance indices of the results obtained by three PET methods against the reference method is shown in Table 4.3. The RMSE, MAE, and R^2 are used to calculate the variation in errors. As shown in Figure 4.12, SPEI values are nearly identical, regardless of the PET calculation method. Slight differences in a few years cannot be considered significant despite differences; drought severity remains the same in all cases. SPEI is calculated for 12, 6, and 3-month time scales. The 6-month time scale distinguishes between summer and winter periods.

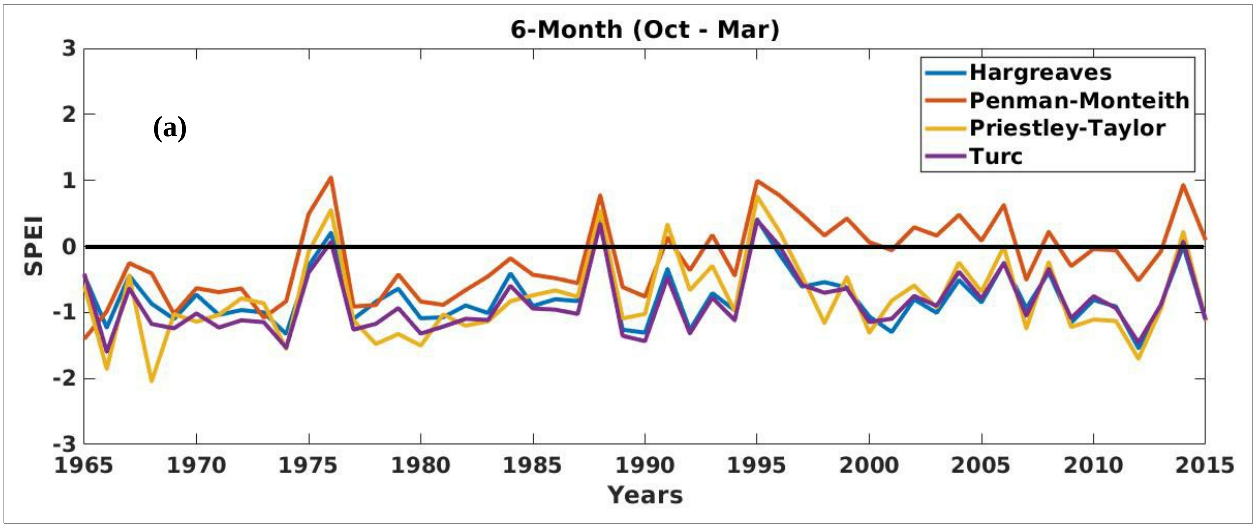

Figure 4.13: SPEI values calculated for the 6-month period (Oct – Mar)

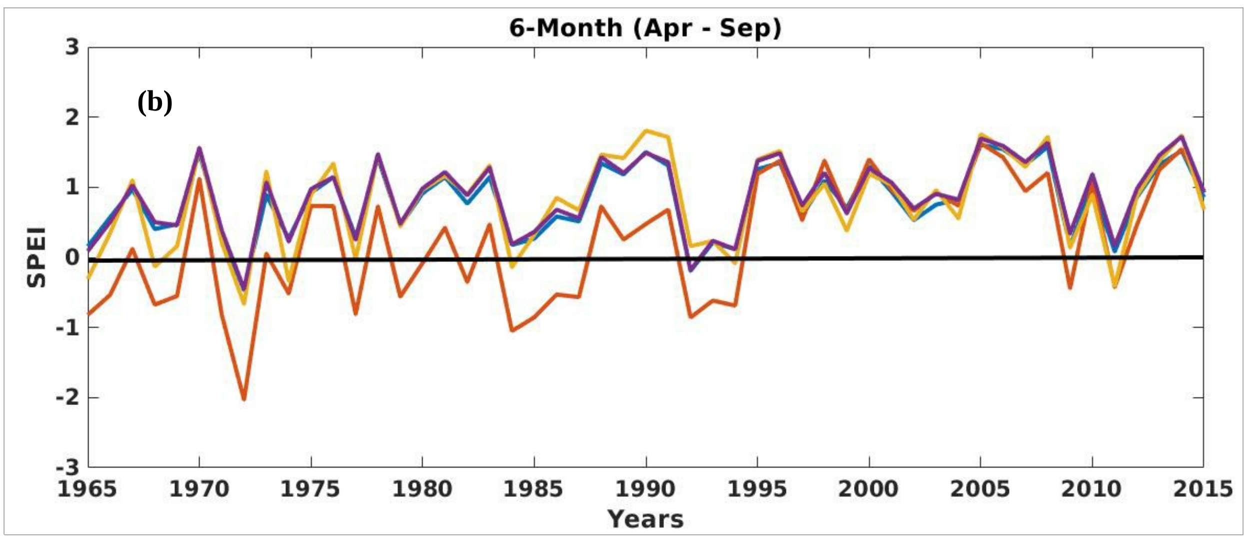

Figure 4.14: SPEI values calculated for the 6-month periods (Apr - Sep)

Table 4.4: Performance statistical indicators of SPEI values calculated by various PET methods against the reference method for the 6-month periods (October - March, April - September)

6-month period, October - March

Method	RMSE (mm)	MAE (mm)	R^2
Hargreaves	0.717	0.574	0.61
Priestley-Taylor	0.743	0.592	0.55
Turc	0.706	0.579	0.65

6-month period, April - September

Method	RMSE (mm)	MAE (mm)	R^2
Hargreaves	0.732	0.558	0.78
Priestley-Taylor	0.787	0.597	0.66
Turc	0.768	0.562	0.77

The results for the 6-month period October - March and April - September are shown in Figure 4.13 and 4.14, and the RMSE, MAE, and R^2 values are shown in Table 4.4. From Figure 4.13, 4.14 and Table 4.4, it can be concluded that the SPEI value produced by the three different PET methods are not identical to those produced by the reference method as expected; deviations occurred in a 6-month period compared to the annual period. Such deviations may be due to SPEI values calculated over shorter time scales is more sensitive to short-term variations in precipitation and evapotranspiration compared to longer time scales. Shorter time scales capture fluctuations in weather patterns and climate conditions and effects of precipitation and evapotranspiration will be influenced by previous and future periods resulting in deviations. The same analysis is done for a 3-month period (Oct-Dec, Jan - Mar, Apr-Jun, Jul - Sep). The 3-month SPEI are shown in Figure 4.15 to 4.18, and statistical parameters are shown in Table 4.5.

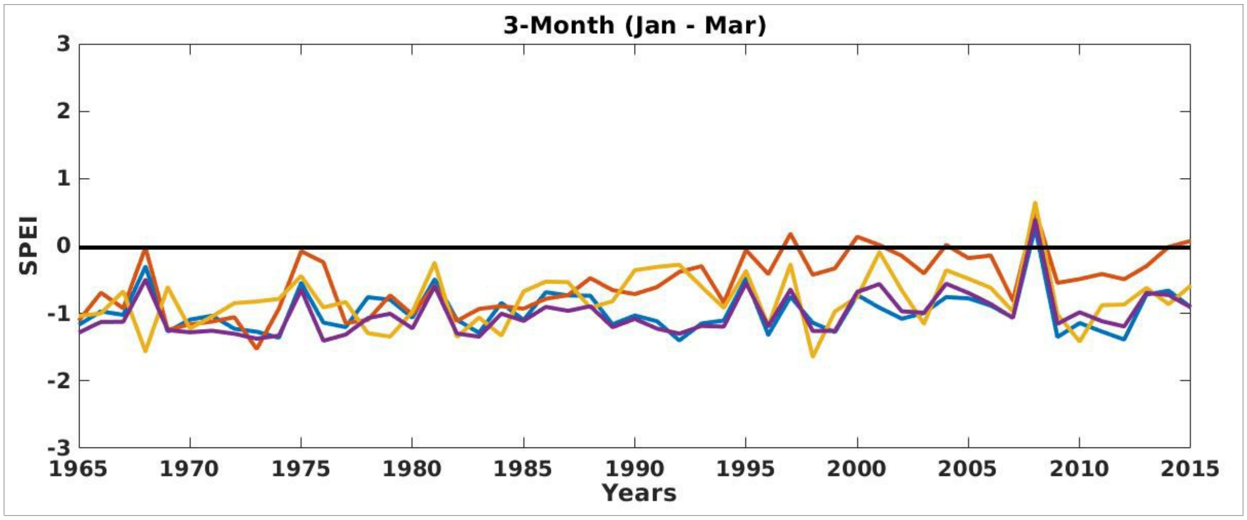

Figure 4.15: SPEI values calculated for the 3-month period (Jan - mar)

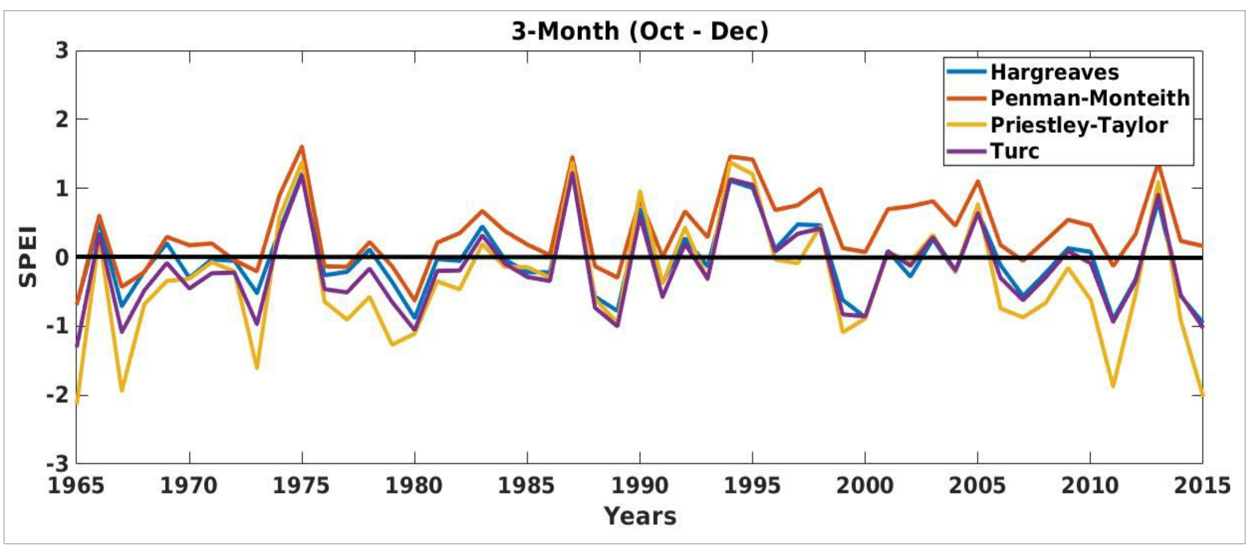

Figure 4.16: SPEI values calculated for the 3-month period (Oct - Dec)

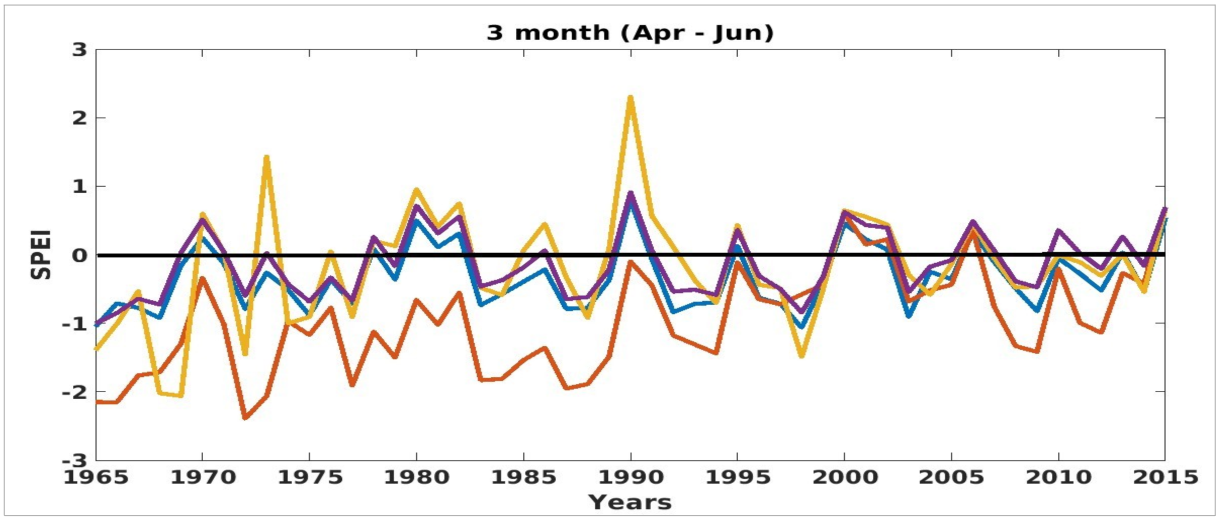

Figure 4.17: SPEI values calculated for the 3-month period (Apr - Jun)

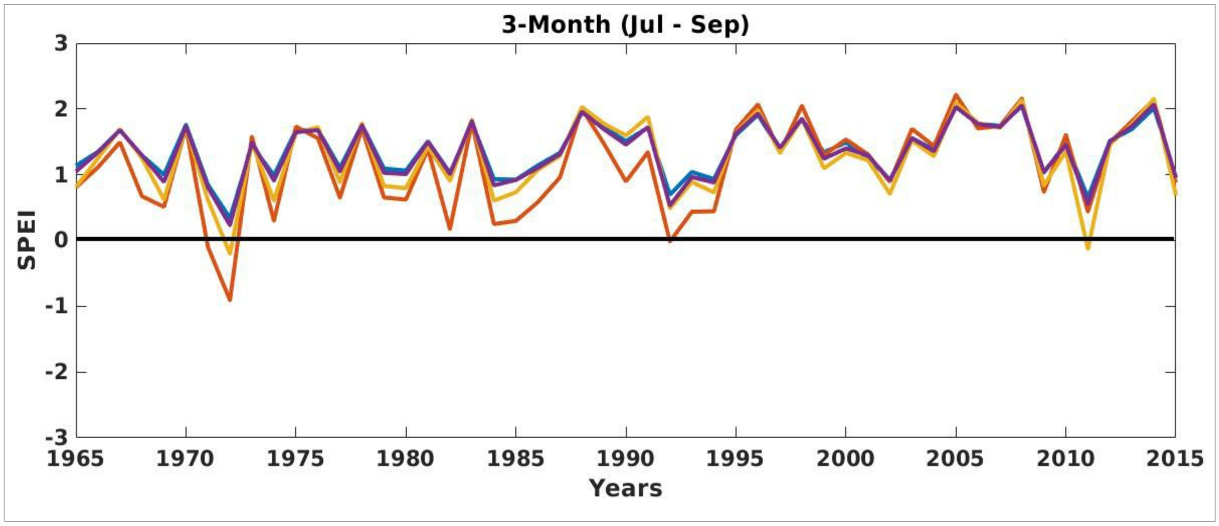

Figure 4.18: SPEI values calculated for the 3-month period (Jul - Sep)

Table 4.5: Performance statistical indicators of SPEI values calculated by various PET_o methods against the reference method for the 3-month periods (October - December, January - March, April - June, July - September)

3-month period, October - December

Method	RMSE (mm)	MAE (mm)	R^2
Hargreaves	0.476	0.405	0.79
Priestley-Taylor	0.808	0.675	0.77

Turc	0.566	0.531	0.90

3-month period, January - March

Method	RMSE (mm)	MAE (mm)	R^2
Hargreaves	0.563	0.416	0.30
Priestley-Taylor	0.610	0.539	0.19
Turc	0.545	0.455	0.54

3-month period, April - June

Method	RMSE (mm)	MAE (mm)	R^2
Hargreaves	0.83	0.63	0.48
Priestley-Taylor	1.10	0.89	0.25
Turc	0.97	0.67	0.52

3-month period,July - September

Method	RMSE (mm)	MAE (mm)	R^2
Hargreaves	0.407	0.229	0.89
Priestley-Taylor	0.412	0.271	0.83
Turc	0.373	0.204	0.90

Figures 4.15 to 4.18 and Table 4.5 show that SPEI values produced by different PET methods are not identical to the Penman-Monteith method. The effect of the PET method on SPEI values is small. However, there are some significant deviations for shorter timescale droughts such as at 3 and 6 months SPEI values. Some variations exist, as observed in the January - March, and April - June periods. In other cases, the results are satisfactorily close to the reference period.

4.6 Conclusions

The daily PET over semi-arid climatic conditions over Hyderabad, Telangana, India, was modeled using the empirical and data-driven model. The daily PET was estimated with the ANN modeling technique using four input variables as maximum and minimum air temperatures, relative humidity and solar radiation, and wind speed; three input variables as average air temperature, relative humidity, and solar radiation; two input variables as temperature and solar radiation. The results were discussed with the results of alternative methods of PET calculation, such as the combination-based method of Penman-Monteith, the radiation-based methods of Priestly-Taylor, the temperature-based methods of Hargreaves, and the Turc method. The correlation coefficient values suggest that temperature is the most important factor, followed by solar radiation, wind speed, and relative humidity. ANN with all-climate variables as input simulated PET values estimated using the Penman-Monteith method. Temperature and solar radiation have a maximum correlation with PET estimates of Penman-Monteith models as compared to relative humidity and wind speed. The Turc model uses temperature and solar radiation as input variables and has high accuracy with the ANN model. From the figure 4.11, it is concluded that relative humidity has the less dependency on PET estimates compared to other input variables. The Priestly-Taylor model considers relative humidity, temperature, and solar radiation input variables. Due to the lower relative humidity dependency on the reference PET estimates, the Priestly-Taylor model has lower accuracy with ANN than the Turc model. The study concludes that the empirical models work well with data-driven algorithms that consider the climate variables highly dependent on the standard reference PET estimates. Such studies can be implemented to develop data-driven models statistically dependent on reference model PET estimates.

Further, it can be concluded that when a parameter or an input variable with a lower correlation is added to the set of features for training over ANN, prediction accuracy will be decreased. The results showed that ANN provides good agreement with the PET obtained by the Penman-Monteith method. The study demonstrated that modeling PET through the ANN technique gave better estimates that proved their performance criterion, i.e., R^2 as 0.96. The study concludes that the models performance varies according to the number of inputs and the predicted time step. Overall, results are of significant practical use when limited climate data is available to estimate the PET. Penman-Monteith method correlated better with ANN model as the values of R^2, RMSE, and MAE are 0.97, 0.02, and 0.008 respectively. Hargreaves and Turc also correlated comparatively better than Priestley-Taylor method. Further, to study the impact of these methods on drought estimation, SPEI is calculated at 12, 6, and 3-month time scales for all methods. Penman-Monteith model estimates of SPEI are considered the standard reference method. All other methods are compared with the reference method using RMSE, MAE, and R^2. It is shown that no significant influence on the results of SPEI was detected by three PET methods (Hargreaves, Priestley-Taylor, and Turc). Regardless of the reference period, some deviations occurred in the 3-month period of (Jan - Mar) and (Apr-Jun) for the Priestley-Taylor method. The study shows that SPEI can be reliably assessed for various timescales even if the minimum data is available. Hargreaves and Turc method correlated better with the FAO Penman-Monteith method. The Turc model performed marginally better than the Hargreaves. Thus, the present study concludes the selection of Hargreaves and Turc models will give a good indication of drought events. These two methods Hargreaves and Turc PET also correlated better with data driven model. Penman-Monteith gives best results but it requires many input variables to compute. Hence, present study concludes to use Hargreaves and Turc methods for PET and drought estimation when minimum data is available. Here in this chapter, the effect of PET methods on the drought indices is studied for Hyderabad station. Furthermore, to study the effect of AET, which is another promising variable in the drought assessment in capturing actual water availability in the drought assessment, the study extended to implemented hydrological model and remote sensing based PET and AET estimates at catchment scale as explained in the Chapter 5. The study used empirical and SWAT model to estimate both PET and AET estimates, which can be enforced into the drought indices of SPEI and SPAEI, implemented with Tunga-Bhadra catchment which is discussed in Chapter 5.

Chapter 5

Drought Analysis using different potential and actual evapotranspiration methods for the Tunga-Bhadra catchment, India

5.1 Introduction

To assess the drought events accurately by the various drought indices it is necessary to predict the hydro-meteorological variables (PET and AET) precisely. There are several challenges in estimating AET and

PET at the fine spatial resolution. There are various empirical models (Budyko, Penman-Monteith, Hargreaves, and Turc) for estimating AET and PET. Still, these empirical methods does not account for the catchment characteristics, which may underestimates the actual amount of hydrological variables. Further, satellite-based remote sensing data are accessible for extracting evapotranspiration (ET) values. It provides global coverage and continuous observations of land surface variables affecting ET. Another conceptual based approach to estimate PET and AET at catchment scale is hydrological model such as SWAT. The present study aimed to include various approaches of empirical (Budyko, Penman-Monteith, Hargreaves, and Turc), modeled (SWAT), and remote sensing in the drought characterization using SPEI and SPAEI. Remote sensing PET and AET is considered as standard method to compare both empirical and modeled PET and AET estimates. The present methodology was tested on a dry-sub-humid river catchment of India, the Tungabhadra River catchment.

5.2 Methods

The methodological approach of the present research work consists of two major analytical parts. Estimation of hydro-meteorological variables by different models and drought assessment with standardized drought indices, SPEI, and SPAEI (Fig. 5.1). In this study, it is focused on the generation of PET and AET by various techniques to identify the drought events using SPEI and SPAEI drought index. In the first part of the analysis, three approaches were chosen, i.e., empirical models, physically-based distributed model (SWAT), and remote sensing datasets for the simulation of PET and AET for the Tunga-Bhadra catchment. The climate data, such as precipitation, atmospheric temperature, and solar radiation, is utilized for estimating PET and AET by Empirical models (such as Hargreaves, Penman-Monteith, Budyko, and Turc). Further, spatial data Digital elevation Model (DEM data) with Land Use Land Cover and Soil data is utilized in QSWAT for catchment delineation. With the climate inputs, the data model is set up to run and calibrate with the observed streamflow data. The calibrated model was used to extract hydro-meteorological variables to formulate SPEI and SPAEI. Furthermore, Satellite-based remote sensing data, i.e., Moderate Resolution Imaging Spectroradiometer (MODIS) evapotranspiration data sets (PET and AET), were downloaded and utilized for SPEI and SPAEI formulation. MODIS data is downloaded from Appeears (https://appeears.earthdatacloud.nasa.gov) website. In the second part of this study, SPEI and SPAEI index drought indices are formulated using the hydro-meteorological variables estimated by different models and analyzed its results for the various models. The estimation of hydro-meteorological variables using empirical equations and its simulation by SWAT, drought index formulation, and analysis over the period is explained in the section below, along with the comparative analysis of various model results.

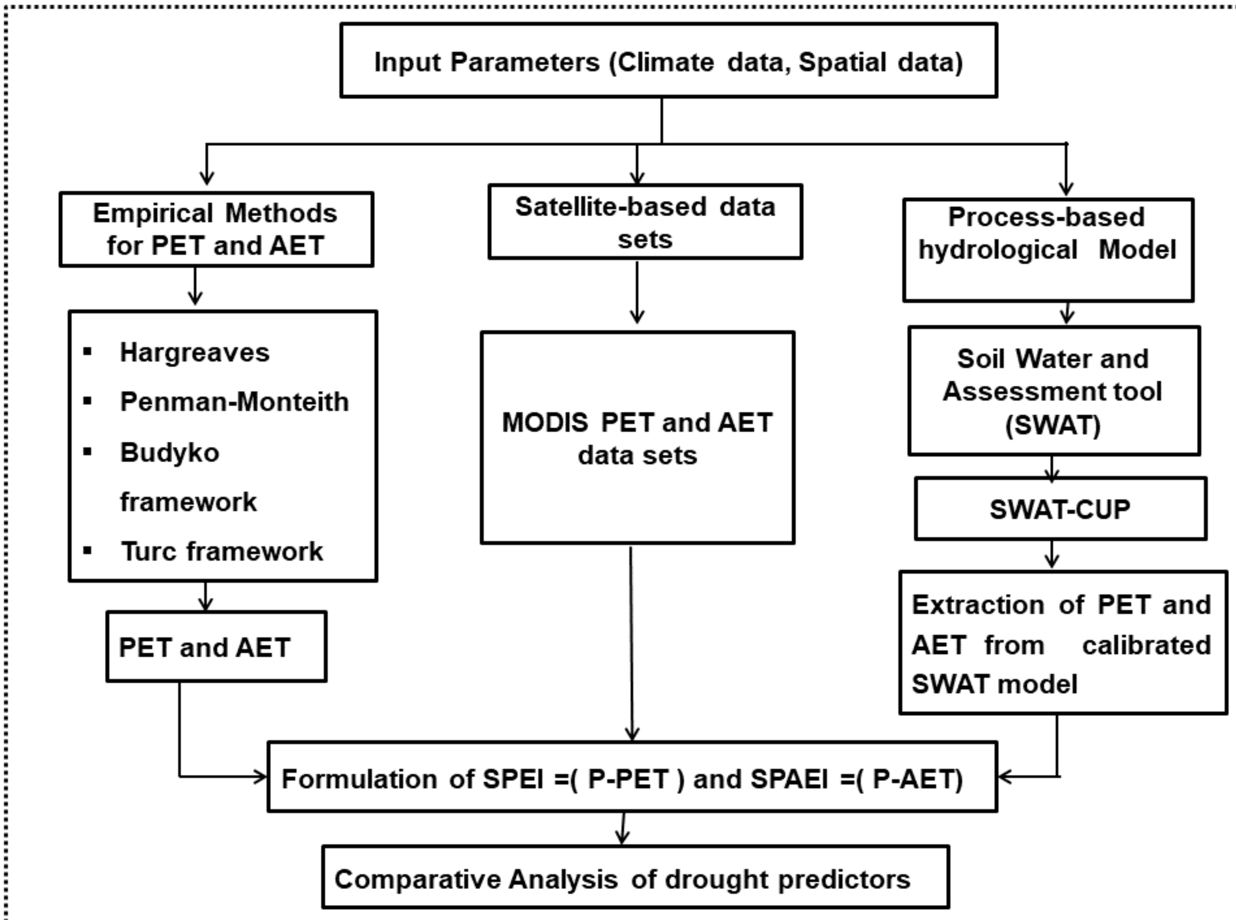

Figure 5.1. Schematic diagram of the workflow

5.2.1 Estimation of Hydro-meteorological variables by different approaches

In this work, PET and AET are calculated using three methods: Empirical, Modeled and remote sensing. The first is to use empirical formulae. There are several equations for the formulation of PET among all FAO-56 Penman-Monteith [32], which was adopted as the standard procedure for PET by the International Commission of Irrigation and Drainage (ICID), the Food and Agriculture Organization of the United Nations (FAO), and the American Society of Civil Engineers (ASCE), and Hargreaves Method, which is chosen to formulate PET and their comparative analysis due to its minimum data requirement. AET was also estimated using the Budyko and Turc frameworks. SWAT was used to simulate PET and AET in the second approach, and in the third approach, these were retrieved from remote-sensing-based satellite data sources (MODIS). The empirical equations and SWAT model setup is explained in the section below.

5.2.2 Estimation of PET and AET by Empirical Methods

PET is estimated using Penman-Monteith and Hargreaves methods. Equations for these methods are given in Chapter 4.

AET by Budyko Method

The Estimation of AET is based on the water availability in terms of precipitation (P) and estimated PET by Penman-Monteith as the International Commission adopted it on Irrigation and Drainage (ICID) and the American Society of Civil Engineers (ASCE) as the standard procedure for PET. In this context, this study used empirical models which work on the assumption that AET is limited by water availability in terms of precipitation under very dry conditions and available energy under very wet conditions in terms of PET [40], [41]. Budyko (1958) developed a relationship between three hydro-meteorological variables, P, PET, and AET (Eq.5.1), which states that the ratio of the AET over precipitation (AET/P) is fundamentally related to the ratio of the PET over precipitation (PET/P) [40], [63] as follows:

$$\frac{AET}{P} = 1 + \frac{PET}{P} - ¿¿ \qquad (5.1)$$

Where the parameter 'ω' accounts for the basin characteristics such as soil, vegetation, terrain, etc. The original Budyko equation has been modified by several researchers (e.g., [64] and one of the widely used formulation is implemented by Zhang et al., (2004) for estimating the AET for the Tunga-Bhadra catchment as follows

$$AET_{Budyko} = ¿ \qquad (5.2)$$

AET by Turc method

Turc method uses precipitation, PET, and soil and vegetative characteristics implicitly. It is one of the widely used hydrological equations [38]

$$AET_{Turc} = \frac{P}{\sqrt{0.9 + \frac{P^2}{PET^2}}}$$

(5.3)

Where P is the precipitation, and PET is potential evapotranspiration. The present study used Penman-Monteith PET for calculating AET, as it is considered a standard method.

5.2.3 Simulation of Hydro-meteorological variables by SWAT

Soil and Water Assessment Tool, SWAT, is a physically-based distributed hydrological model that simulates the flow of a larger river. The water balance equation governs the land phase of the hydrologic cycle in SWAT (5.4). The fundamental unit of the SWAT model is the hydrologic response unit (HRU). HRUs are allocated based on land use, land cover, soil type, and slope of the area. These three factors are vital in defining the HRU of an area. Dividing the whole catchment into discrete watersheds will simplify analyzing the characteristics of watersheds. Overall, the SWAT model includes all the details required for river basin management.

$$SW_t = SW_o + \sum_{i=1}^{N} \left(R_{day} - Q_{surf} - E_a - W_{seep} - Q_{gw} \right) \tag{5.4}$$

Where SW_t is Soil-water content, SW_o is the initial soil water content, R_{day} is amount of Precipitation, Q_{surf} is Surface runoff, E_a is Evapotranspiration, W_{seep} is water entering the vadose zone from the soil profile, and Q_{gw} is Return flow.

For model setup, QSWAT with SWAT Editor 2012 is used to model the hydro-meteorological variables of PET, AET, and discharge of the Tunga-Bhadra river catchment. Shuttle Radar Topography Mission (SRTM) Digital elevation Model (DEM) generates the stream networks [65] and delineates the catchment area in the QSWAT.

Precipitation, atmospheric temperature, wind velocity, solar radiation, and relative humidity data are used as model input. SWAT Calibration and Uncertainty Program (SWAT-CUP) is an interface that was developed for SWAT. Using this calibration, uncertainty or sensitivity analysis is performed [66]. The model performance was based on two objective functions: Nash-Sutcliffe Efficiency and Coefficient of determination, R^2. The present study conducted a multi-gauge calibration technique to obtain monthly streamflow for the catchment area. The SWAT model was set up for 1986-2013, starting 2 years as a warm-up period. However, in this study, our analysis of drought is from 2000 to 2013.

Further, these SWAT simulated hydro-meteorological variables are compared with the calculated values by empirical model and the satellite datasets; Standardized drought indices are computed for the drought studies using hydro-meteorological variables extracted by various approaches are discussed in the section below.

5.2.4 Assessment of Meteorological drought by SPEI and SPAEI

SPEI takes both precipitation and PET into account, it combines the response of drought to evapotranspiration. The SPEI is calculated based on the probability that the differences between precipitation and PET are not exceeded and adjusted using a three-parameter Log-logistic. Whereas SPAEI is calculated based on the probability that the difference between precipitation and AET. Both are calculated at a 12-month time scale. The SPEI and SPAEI at different time scales represents different climatic water balances. Equations used to calculate SPEI are discussed in chapter 4. The structure of SPEI is considered to formulate SPAEI also with the inclusion of AET in the place of PET. That is for SPAEI is restructured with (P-AET) instead of (P-PET) as explained in Chapter 4.

5.2.5 Evaluation metrics

The accuracy of the models is validated using Nash-Sutcliffe efficiency (NSE) and Coefficient of determination (R^2).

$$\text{NSE} = 1 - \sum_i ¿¿¿¿ \qquad (5.5)$$

$$R^2 = 1 - \frac{\sum_i \left(O_i - \widehat{O}_i\right)^2}{\sum_i \left(O_i - \acute{O}\right)^2}$$

(5.6)

Where O_i is the observed values, $O_{i,\sim¿¿}$ is the simulated values, and $\acute{O}$ is the mean value of O

5.3 Results and Discussions

5.3.1 Variation of Precipitation and Streamflow at Catchment

The annual precipitation and streamflow values extracted from the SWAT model are graphically shown in Fig. 5.2 for the Tung-Bhadra river catchment. Annual precipitation varies from 720 mm to 1453 mm, whereas annual streamflow ranges from 3200-8250 cumecs of the Tunga-Bhadra catchment from 1988 to 2013. A continual drop in precipitation is observed between 2000-2004 (Fig.5.2), with the falling profile of streamflow in the same year, which specify a severe drought over the catchment area. These years were also considered as major long-term drought years in India [67], [68]. The percentage of fall in streamflow that is considered as drought will depend on different factors, including location, climate, and hydrological conditions. However, a commonly used threshold is a decrease in streamflow by 10 to 30% [69]

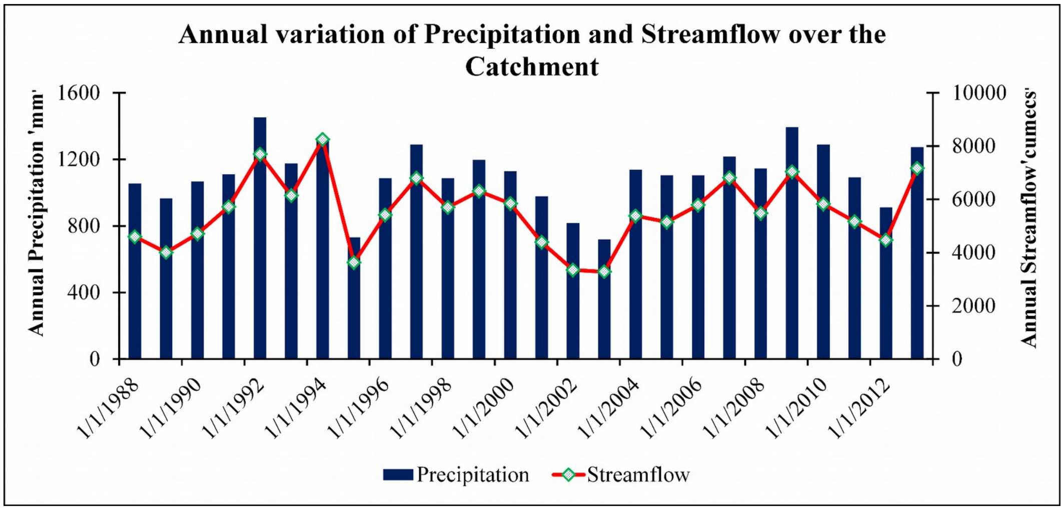

Figure 5.2 Variation of Precipitation and Streamflow over Tunga-Bhadra river catchment

5.3.2 Comparative Analysis of PET and AET by various Empirical models, Remote sensing, and SWAT over the Catchment

The analysis of the catchment area of PET and AET is from 2000 to 2013. Figure 5.3 shows the comparative plots of monthly PET over the Tunga-Bhadra catchment. Remote sensing-based PET ranges from 86.5 mm to 257.7 mm, SWAT simulated PET 56.9 mm to 272.8 mm, Hargreaves PET 62.9 mm to 207 mm, whereas Penman-Monteith PET 55.5 mm to 239.5 mm. There is a significant variation in the lowest value of PET

estimated by Hargreaves equations and remote-sensing-based PET compared to SWAT and Penman-Monteith PET. However, the maximum monthly value estimated by the Hargreaves equation has shown a large deviation with remote sensing and SWAT modeled PET of 50 mm and 65 mm, respectively, which can show possible deviation in the identification of drought severity with any drought indices.

Further, significant variation is also observed in AET (Figure 5.4). AET estimates by Budyko range from 0 to 118.9 mm, Turc AET from 0 to 124.5 mm, SWAT modeled AET ranges from 7 mm to 145 mm, and remote sensing AET varies from 7 mm to 94.5 mm.

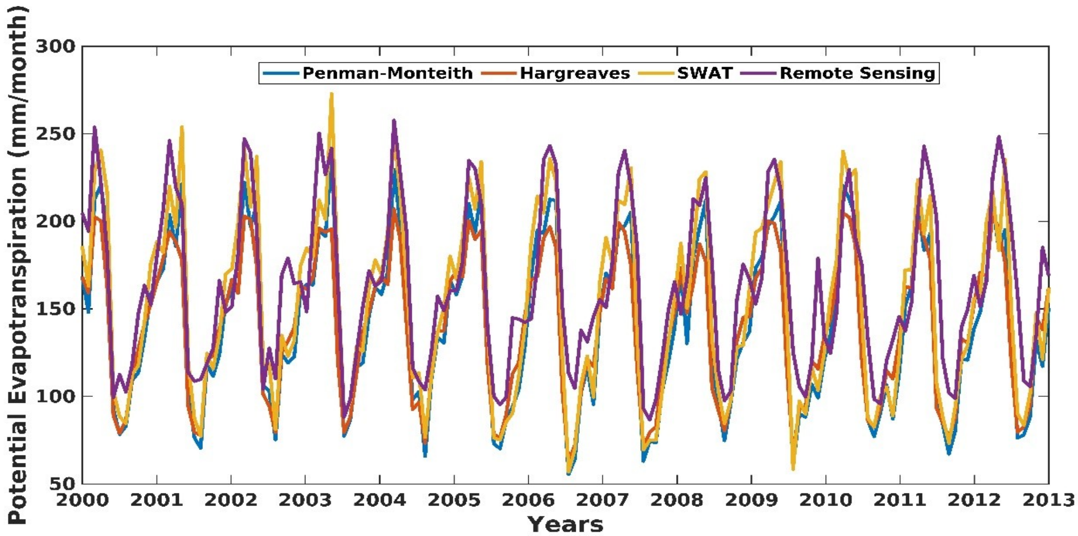

Figure 5.3: Comparative plot of monthly estimated PET values by SWAT, Remote Sensing, Penman-Monteith and Hargreaves method

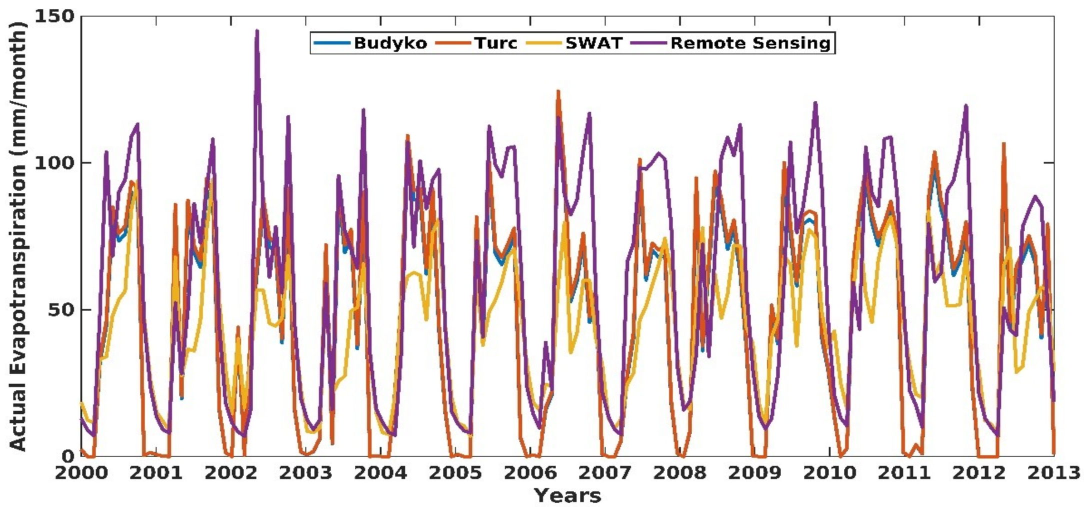

Figure 5.4: Comparative plot of monthly estimated AET values by SWAT, Remote Sensing, Budyko and Turc framework

Table 5.1: Performance statistical indicators of PET values calculated by various methods against the remote sensing method.

Method	NSE	R^2
Penman-Monteith	0.52	0.78

Hargreaves	0.51	0.76
SWAT	0.61	0.74

Table 5.2: Performance statistical indicators of AET values calculated by various methods against the remote sensing method.

Method	NSE	R^2
Budyko	0.50	0.65
Turc	0.52	0.65
SWAT	0.43	0.63

Table 5.1 and 5.2 shows the comparative analysis of PET and AET estimates against the reference method, which is the remote sensing method. In this study, the remote sensing method is considered a standard method as it is satellite-based data. Satellite-based data partially solve the problem by providing information in a fast and cost-effective way. The results show that PET and AET values produced by different methods are not identical to the reference method.

5.3.3 A Comparative Assessment of drought by SPEI and SPAEI using Empirical, SWAT, and Remote Sensing models

Despite that there is a large variation in generated PET and AET, it is observed that the average value of drought indices formulated by using the generated PET and AET by various methods are nearly the same (Fig. 5.5 and 5.6) with the values of -1.20 (SPEI) and -1.22 (SPAEI) for the major drought event period 2002 to 2004. However, a longer duration of drought event is captured by the SPEI index, which is formulated using SWAT simulated PET in comparison to other PET-based indices (Fig. 5.7). At the same time, SPAEI estimated by all four approaches, that is, SWAT, remote sensing, budyko, and turc method captures the event with nearly same duration (Fig. 5.8). It has been seen that budyko and turc approach predicts the onset and ends of drought in a similar way.

AET estimated by SWAT, empirical equations, and remote sensing does not affect more than one month in the detection of an event by SPAEI, i.e., the start and the end of one drought event. Whereas PET estimates show the larger effect in the detection of the termination period of the event by SPEI.

SPEI formulated by SWAT-PET terminates the drought event by 15 months; this may be because of a sudden rise of climatic factors captured by SWAT.

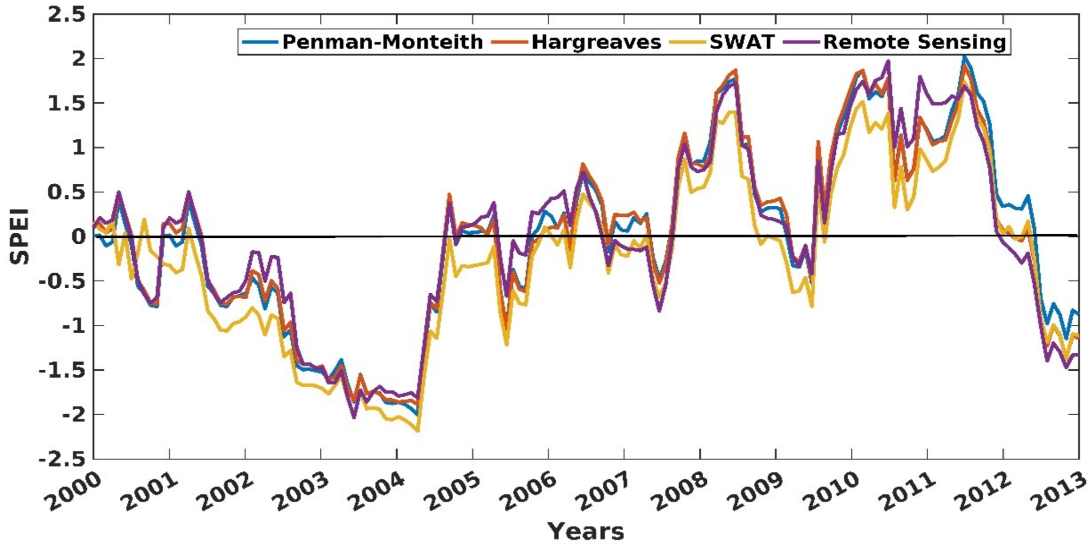

Figure 5.5: Variation of SPEI drought index using various PET estimates

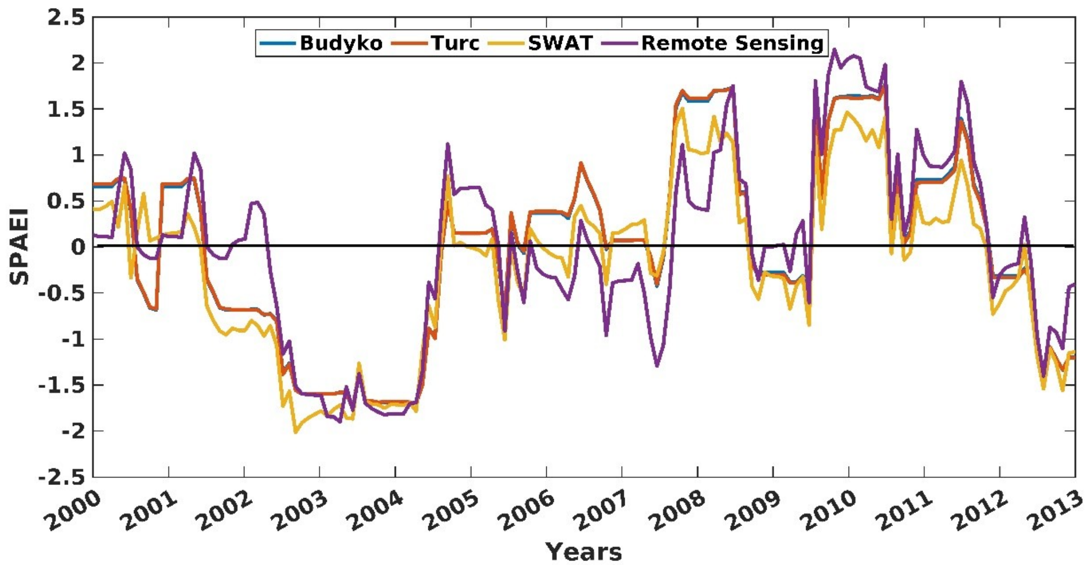

Figure 5.6: Variation of SPAEI drought index using various AET estimates

Table 5.3: Performance statistical indicators of SPEI values calculated by various methods against the remote sensing method

Method	NSE	R^2
Penman-Monteith	0.93	0.93
Hargreaves	0.95	0.95

SWAT	0.85	0.91

Table 5.4: Performance statistical indicators of SPAEI values calculated by various methods against the remote sensing method

Method	NSE	R^2
Budyko	0.75	0.77
Turc	0.74	0.76
SWAT	0.71	0.75

Table 5.3 and 5.4 shows the comparative analysis of drought indices SPEI and SPAEI against the reference method, where satellite-based PET and AETs were used in the drought indices estimation. By these results, it can be concluded that despite the variations in PET and AET estimates, drought indices values are nearly the same. SPEI values are nearly identical, regardless of the PET and AET calculation method.

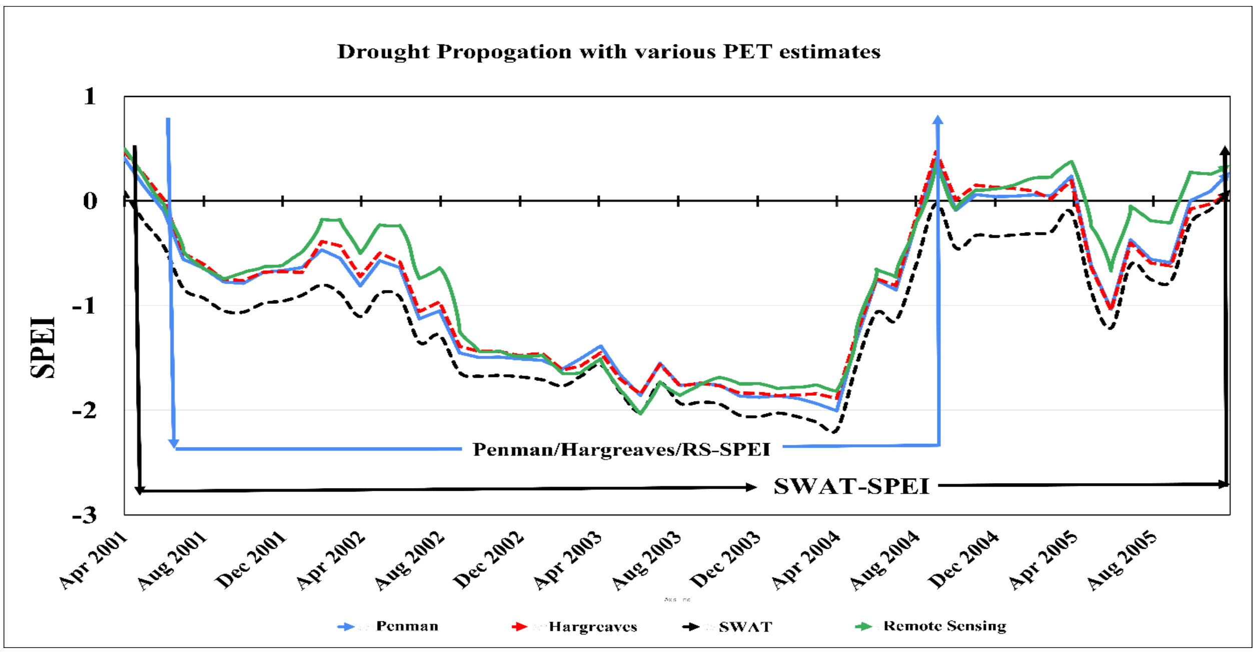

Figure 5.7: Drought onset and termination month identified by SPEI drought index by using various PET estimates for the major drought event periods (2002-2004)

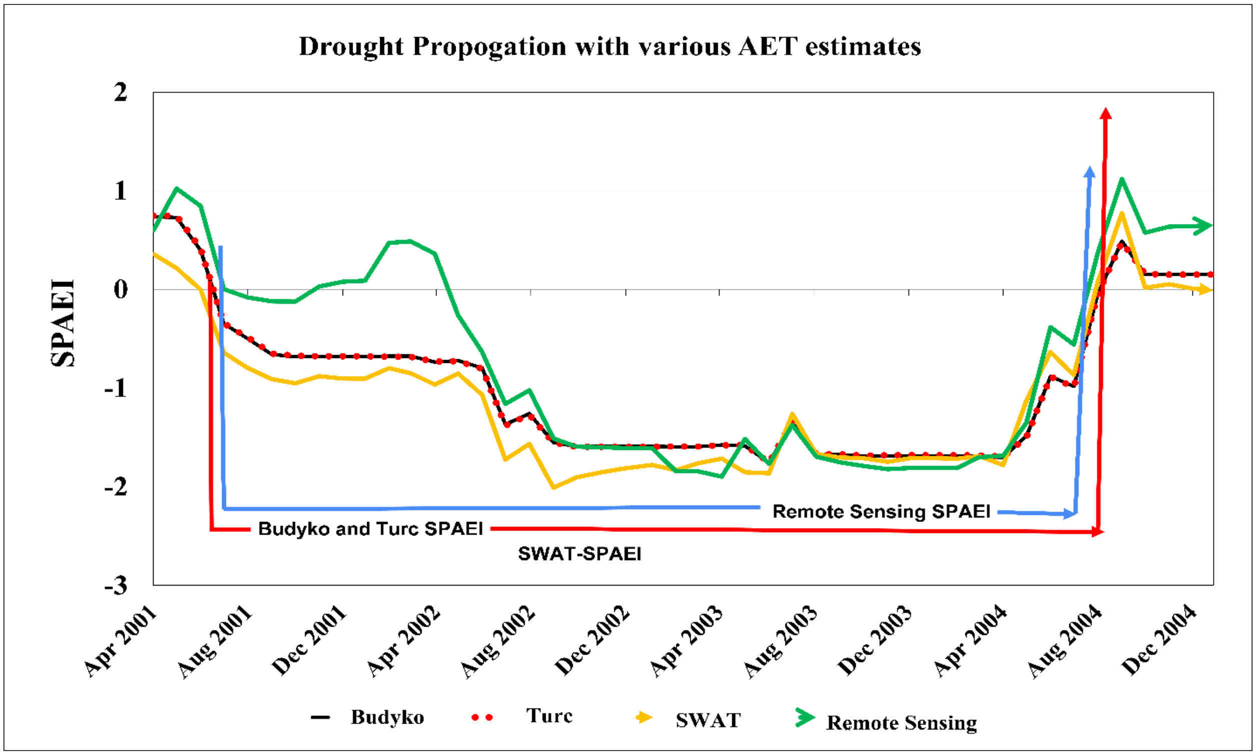

Figure 5.8: Drought onset and termination month identified by SPAEI drought index by using various AET estimates for the major drought event periods (2002-2004)

5.3.4 Drought Characteristics Analysis

In this study, the duration and severity of the drought were analyzed. When SPEI values go below zero, or at a time when SPEI values are negative, a drought event is said to have occurred. The length of the period during which the SPEI value is consistently negative is the duration of the drought (D). It begins when the SPEI values are equal to -1 and ends when they become positive. The cumulative SPEI values throughout the droughts duration determine the drought severity (S). which is defined by

$$S = -\sum_{i=1}^{D} SPEI_i \qquad (5.7)$$

The total number of drought events that occurred for PET estimates using Penman-Monteith, Hargreaves, SWAT, and Remote Sensing are 11, 9, 13, and 7, respectively from Jan 2000 to Dec 2012. Major drought events occurred using Penman-Monteith from Jun 2001 to Aug 2004 with a severity value of -46.93. Using Hargreaves, a major event occurred from Jul 2001 to Aug 2004 with a severity value of -45.60. using SWAT, a major event occurred from May 2001 to Nov 2005 with a severity value of -62.89. and using remote sensing, the major event occurred from Jun 2001 to Aug 2004 with a severity value of -43.22.

And similarly, for AET total number of drought events using Budyko, Turc, SWAT, and Remote sensing are 8, 8, 13, and 12, respectively from Jan 2000 to Dec 2012. Major drought events occurred using Budyko from Jul 2001 to Aug 2004 with a severity value of -46.53. Using Turc, a major event occurred from Jul 2001 to Aug 2004 with a severity value of -46.48. Using SWAT, the major event occurred from Jun 2001 to Jul 2004 with a severity value of -51.64. using remote sensing, the major event occurred from May 2002 to Jul 2004 with a severity value of -39.48.

5.4 Conclusions

This study aimed to do drought analysis using different PET and AET models for the Tunga-Bhadra catchment, India, from 2000 to 2013. PET is estimated using empirical methods of Penman-Monteith and Hargreaves. AET is estimated using empirical methods of Budyko and Turc. The hydrological method SWAT is used to estimate both PET and AET. Remote Sensing (MODIS) data for PET and AET is downloaded from the Appeears website. There is a significant variation in the lowest value of PET estimated by Hargreaves equations and remote-sensing-based PET compared to SWAT and Penman-Monteith PET. However, the maximum monthly value estimated by the Hargreaves equation has shown a large deviation with remote sensing and SWAT modeled PET. For the study area, continual drop in precipitation was observed between the years 2000-2004, with the falling profile of streamflow in the same year, which specifies major drought events that occurred in those years. After estimating both PET and AET, drought is estimated using SPEI and SPAEI. The drought indices values are compared with remote sensing-based drought indices. Results show that despite variations observed in PET and AET estimates, drought indices values are nearly identical regardless of the method. It is observed that the average value of drought indices formulated by using the generated PET and AET by various methods are nearly the same with the values of -1.20 (SPEI) and -1.22 (SPAEI) for the major drought event period 2002 to 2004. Although all methods correlated better with each other, Hargreaves for SPEI and Budyko for SPAEI performed relatively better with NSE, R^2 values of 0.95, 0.95, and 0.75, 0.77, respectively. The total number of drought events that occurred for PET estimates using Penman, Hargreaves, SWAT, and Remote Sensing are 11, 9, 13, and 7 respectively. Long duration of drought using PET is captured by SWAT with a severity value of -62.89 from May 2001 to Nov 2005. All other three methods generated similar severity values.

And similarly, for AET total number of drought events using Budyko, Turc, SWAT, and Remote sensing are 8, 8, 13, and 12, respectively. The long duration of drought using AET is captured by SWAT with a severity value of -51.64 from Jun 2001 to Jul 2004. Budyko and Turc approach predicts the onset and end of the drought similarly. It is recommended to use PET instead of AET when estimating drought indices as SPEI values performed relatively better than SPAEI. However this conclusion may not be universally applicable, as the performance of drought indices can vary depending on the specific characteristics of the study area, data quality and climatic conditions. Although PET and AET estimates vary with different models, drought indices SPEI and SPAEI are not differing much. Hargreaves and Penman-Monteith performed better results compared to reference method in SPEI calculations. And for SPAEI Budyko and Turc performed better results. Thus, the present study concludes that empirical models correlated better with the remote sensing data.

Chapter 6

Summary and Conclusions

The study aimed to simulate the complex PET and AET processes using empirical (Penman-Monteith, Hargreaves, Priestley-Taylor, Budyko and Turc), data-driven (ANN) and hydrological model (SWAT). Further, the thesis aimed to study the uncertainty in the drought characterization of SPEI and SPAEI using various PET and AET estimates implemented on Hyderabad and Tunga-Bhadra River basin, India. The input variables used for PET estimates are temperature, relative humidity, wind speed, and solar radiation. Data-driven model ANN is used to estimate PET using these climate input variable combinations. ANN results are compared with the results of alternate PET methods. Penman-Monteith method correlated better with ANN model. Hargreaves and Turc also correlated comparatively better than Priestley-Taylor method. Due to the lower relative humidity dependency on the PET estimates, the Priestly-Taylor model has lower accuracy with ANN.

Further, to study the impact of various PET methods on drought estimation, SPEI is calculated at 12, 6, and 3-month time scales. Penman-Monteith model estimates of SPEI are considered the standard reference method. All other methods are compared with the Penman-Monteith method using RMSE, MAE, and R^2. It is shown that no significant influence on the results of SPEI was detected by three PET methods (Hargreaves, Turc, and Priestley-Taylor). Uncertainty in the drought indices was noted in the 3-month period of (Jan - Mar) and (Apr-Jun) for the Priestley-Taylor method. Hargreaves and Turc methods correlated better with the standard method of Penman-Monteith model.

Furthermore, the present study aimed to include different PET and AET estimates for Tunga-Bhadra catchment scale from the period of 2000 to 2013 simulated by hydrological model, SWAT. Furthermore, PET is estimated using empirical methods of Penman-Monteith and Hargreaves. AET is estimated using empirical methods of Budyko and Turc. Remote Sensing (MODIS) based data of PET and AET were used as standard method to validate various empirical and modeled data of the present study. After estimating both PET and AET, drought is estimated using SPEI and SPAEI. The drought indices values are compared with remote sensing-based PET and AET induced drought indices. The research findings of the study are summarized as follows:

- Penman-Monteith, Hargreaves, and Turc methods were correlated better with the data driven ANN model with R^2 values of 0.97, 0.96 and 0.94 respectively.

- The study also emphasized the influence of climate variables on PET estimations and found that temperature, solar radiation, and wind speed has more influence than relative humidity.

- SPEI is calculated at different time scales using various PET methods compared with Penman-Monteith method and it is observed that Hargreaves and Turc method performed better than Priestley-method.

- Hargreaves and Turc methods can be useful in estimating drought when the minimum data is available.

- SPEI and SPAEI are calculated using different methods of PET and AET which are empirical, hydrological, and remote sensing keeping remote sensing as standard method to find the uncertainty of evapotranspiration in drought estimation.

- It is observed that average values formulated by using the generated PET and AET by various methods are nearly the same with the values of -1.20 (SPEI) and -1.22 (SPAEI) for the major drought event period 2002 to 2004.

- Long duration of drought using PET is captured by SWAT with a severity value of -62.89 from May 2001 to Nov 2005. Where as for other methods, using Penman-Monteith it was from Jun 2001 to Aug 2004 with a severity value of -46.93. Using Hargreaves it was from Jul 2001 to Aug 2004 with a severity value of -45.60, and using remote sensing it was from Jun 2001 to Aug 2004 with a severity value of -43.22.

- Long duration of drought using AET is captured by SWAT with a severity value of -51.64 from Jun 2001 to Jul 2004. Where as for other methods, using Budyko it was from Jul 2001 to Aug 2004 with a severity value of -46.53. using Turc it was Jul 2001 to Aug 2004 with a severity value of -46.48, and using remote sensing it was from May 2002 to Jul 2004 with a severity value of -39.48

- It was observed that Hargreaves for SPEI and Budyko for SPAEI performed relatively better with NSE, R^2 values of 0.95, 0.95, and 0.75, 0.77, respectively.

- It is recommended to use PET instead of AET when estimating drought indices as SPEI values performed relatively better than SPAEI.

- In the present study it is observed that although PET and AET estimates vary with different models, drought indices SPEI and SPAEI are not differing much, particularly at annual scales. Significant variability can be noted at shorter-time scales of drought assessments.

- Hargreaves and Penman-Monteith performed better results compared to remote sensing method in SPEI calculations. And for SPAEI, Budyko and Turc performed better results. Thus, the present study concludes that empirical models correlated better with the remote sensing data.

- The results suggest that for ungauged river basins, where detailed hydrological data is limited and difficult to implement hydrological models, empirical based PET and AET estimates can be better choice for drought characterization.

Publications

Book Chapters

1. Kumari, P., Vannam, S.C., Shaik, R., Inayathulla, M. (2022). Assessment of Meteorological Drought Using Standardized Precipitation Evapotranspiration Index—Hyderabad Case Study. In: Kolathayar, S., Mondal, A., Chian, S.C. (eds) Climate Change and Water Security. Lecture Notes in Civil Engineering, vol 178. Springer, Singapore. https://doi.org/10.1007/978-981-16-5501-2_20.
2. Ayaz, A., Chandra, S., Mandlecha, P., Shaik, R. (2021). Modelling of Reference Evapotranspiration for Semi-arid Climates Using Artificial Neural Network. In: Majumder, M., Kale, G.D. (eds) Water and Energy Management in India. Springer, Cham. https://doi.org/10.1007/978-3-030-66683-5_7

Conference Papers

1. Sharas Chandra Vannam, Pallavi Kumari, Rehana Shaik, (2021), Estimation of Standardized Precipitation Evapotranspiration Index for different Potential Evapotranspiration models: A case study of Hyderabad, India, International Virtual Conference on Innovative Trends in Hydrological and Environmental Systems (ITHES 2021), Water and Environment Division, Department of Civil Engineering, National Institute of Technology, Warangal, India, April 28-30, 2021.
2. Pallavi Kumari, Sharas Chandra Vannam, Rehana Shaik, M Inayathulla, Assessment of Meteorological Drought using Standardized Precipitation Evapotranspiration Index - Hyderabad Case Study, Virtual Conference on Disaster risk reduction (VCDRR-2021), Civil Engineering for a Disaster Resilient Society, 15-20 March 2021, NITK, NIDM, IWMI, ADRRN, IHRR.

Journals

1. Ayaz, A., Chandra Vannam, S., Kumar Singh, S., Shaik, R. Machine Learning Models for Estimating Actual Evapotranspiration with Limited Data. *Sustainable Earth Review*, 2022; 2(3): 28-46. doi: 10.52547/sustainearth.2022.102799, https://sustainearth.sbu.ac.ir/article_102799.html.
2. Pallavi Kumari, Sharath Chandra Vannam, Shailesh Kumar Singh, Rehana Shaik (2023), Evaluation of Drought using Empirical, Hydrological Modelled and Remote Sensing based Potential and Actual Evapotranspiration Data Over Semi-Arid River Basin of India, Water Resources Management, WARM-D-23-00493, (Under Review)

References

[1] K. Zarafshani, L. Sharafi, H. Azadi, and S. Van Passel, "Vulnerability Assessment Models to Drought: Toward a Conceptual Framework," *Sustainability*, vol. 8, no. 6, Art. no. 6, Jun. 2016, doi: 10.3390/su8060588.
[2] B. Zhang, A. AghaKouchak, Y. Yang, J. Wei, and G. Wang, "A water-energy balance approach for multi-category drought assessment across globally diverse hydrological basins," *Agricultural and Forest Meteorology*, vol. 264, pp. 247–265, Jan. 2019, doi: 10.1016/j.agrformet.2018.10.010.
[3] J. Sheffield, E. F. Wood, and M. L. Roderick, "Little change in global drought over the past 60 years," *Nature*, vol. 491, no. 7424, Art. no. 7424, Nov. 2012, doi: 10.1038/nature11575.
[4] R. C. Deo and M. Şahin, "Application of the Artificial Neural Network model for prediction of monthly Standardized Precipitation and Evapotranspiration Index using hydrometeorological parameters and climate indices in eastern Australia," *Atmospheric Research*, vol. 161–162, pp. 65–81, Jul. 2015, doi: 10.1016/j.atmosres.2015.03.018.

[5] J.-S. Kim, G.-S. Seo, H.-W. Jang, and J.-H. Lee, “Correlation analysis between Korean spring drought and large-scale teleconnection patterns for drought forecasting,” *KSCE J Civ Eng*, vol. 21, no. 1, pp. 458–466, Jan. 2017, doi: 10.1007/s12205-016-0580-8.

[6] D. A. Wilhite and M. H. Glantz, “Understanding: the Drought Phenomenon: The Role of Definitions,” *Water International*, vol. 10, no. 3, pp. 111–120, Jan. 1985, doi: 10.1080/02508068508686328.

[7] S.-Y. Park, C. Sur, J.-H. Lee, and J.-S. Kim, “Ecological drought monitoring through fish habitat-based flow assessment in the Gam river basin of Korea,” *Ecological Indicators*, vol. 109, p. 105830, Feb. 2020, doi: 10.1016/j.ecolind.2019.105830.

[8] H. Hisdal, L. M. Tallaksen, B. Clausen, and E. Peters, “Hydrological Drought Characteristics”.

[9] Y. Wada, L. P. H. van Beek, N. Wanders, and M. F. P. Bierkens, “Human water consumption intensifies hydrological drought worldwide,” *Environ. Res. Lett.*, vol. 8, no. 3, p. 034036, Sep. 2013, doi: 10.1088/1748-9326/8/3/034036.

[10] S. Shahid and H. Behrawan, “Drought risk assessment in the western part of Bangladesh,” *Nat Hazards*, vol. 46, no. 3, pp. 391–413, Sep. 2008, doi: 10.1007/s11069-007-9191-5.

[11] J. Wang, “A numerical testbed for remote sensing of aerosols, and its demonstration for evaluating retrieval synergy from a geostationary satellite constellation of GEO-CAPE and GOES-R - ScienceDirect,” 2014. https://www.sciencedirect.com/science/article/abs/pii/S0022407314001368 (accessed Dec. 17, 2022).

[12] J. Keyantash and J. A. Dracup, “The Quantification of Drought: An Evaluation of Drought Indices,” *Bulletin of the American Meteorological Society*, vol. 83, no. 8, pp. 1167–1180, Aug. 2002, doi: 10.1175/1520-0477-83.8.1167.

[13] N. Salehnia, A. Alizadeh, H. Sanaeinejad, M. Bannayan, A. Zarrin, and G. Hoogenboom, “Estimation of meteorological drought indices based on AgMERRA precipitation data and station-observed precipitation data,” *J. Arid Land*, vol. 9, no. 6, pp. 797–809, Dec. 2017, doi: 10.1007/s40333-017-0070-y.

[14] Vicente-Serrano, “A Multiscalar Drought Index Sensitive to Global Warming: The Standardized Precipitation Evapotranspiration Index in: Journal of Climate Volume 23 Issue 7 (2010),” 2010. https://journals.ametsoc.org/view/journals/clim/23/7/2009jcli2909.1.xml (accessed Nov. 29, 2022).

[15] W. C. Palmer, *Meteorological Drought*. U.S. Department of Commerce, Weather Bureau, 1965.

[16] T. B. McKee, N. J. Doesken, and J. Kleist, “THE RELATIONSHIP OF DROUGHT FREQUENCY AND DURATION TO TIME SCALES,” 1993.

[17] J. Keyantash and J. A. Dracup, “The Quantification of Drought: An Evaluation of Drought Indices,” *Bulletin of the American Meteorological Society*, vol. 83, no. 8, pp. 1167–1180, Aug. 2002, doi: 10.1175/1520-0477-83.8.1167.

[18] S. Rehana and G. Sireesha Naidu, “Development of hydro-meteorological drought index under climate change – Semi-arid river basin of Peninsular India,” *Journal of Hydrology*, vol. 594, p. 125973, Mar. 2021, doi: 10.1016/j.jhydrol.2021.125973.

[19] Niemeyer S, “JRC Publications Repository,” 2008. https://publications.jrc.ec.europa.eu/repository/handle/111111111/27985 (accessed Nov. 29, 2022).

[20] Brown, “The Vegetation Drought Response Index (VegDRI): A New Integrated Approach for Monitoring Drought Stress in Vegetation: GIScience & Remote Sensing: Vol 45, No 1,” 2008. https://www.tandfonline.com/doi/abs/10.2747/1548-1603.45.1.16 (accessed Nov. 29, 2022).
[21] G. Tsakiris, D. Pangalou, and H. Vangelis, “Regional Drought Assessment Based on the Reconnaissance Drought Index (RDI),” *Water Resour Manage*, vol. 21, no. 5, pp. 821–833, May 2007, doi: 10.1007/s11269-006-9105-4.
[22] Hayes, “‘Chapter 12 Monitoring Drought Using the Standardized Precipitation In’ by Michael J. Hayes, Mark D. Svoboda et al.,” 2006. https://digitalcommons.unl.edu/droughtfacpub/70/ (accessed Nov. 29, 2022).
[23] S. Liu, D. Yan, H. Wang, C. Li, B. Weng, and T. Qin, “Standardized Water Budget Index and Validation in Drought Estimation of Haihe River Basin, North China,” *Advances in Meteorology*, vol. 2016, p. e9159532, Jun. 2016, doi: 10.1155/2016/9159532.
[24] M. L. Shelton, *Hydroclimatology: Perspectives and Applications*. Cambridge University Press, 2009.
[25] S. Rehana and N. T. Monish, “Impact of potential and actual evapotranspiration on drought phenomena over water and energy-limited regions,” *Theor Appl Climatol*, vol. 144, no. 1, pp. 215–238, Apr. 2021, doi: 10.1007/s00704-021-03521-3.
[26] A. Dai, “Drought under global warming: a review,” *WIREs Climate Change*, vol. 2, no. 1, pp. 45–65, 2011, doi: 10.1002/wcc.81.
[27] T. Homdee, K. Pongput, and S. Kanae, “A comparative performance analysis of three standardized climatic drought indices in the Chi River basin, Thailand,” *Agriculture and Natural Resources*, vol. 50, no. 3, pp. 211–219, May 2016, doi: 10.1016/j.anres.2016.02.002.
[28] X. Liu, P. He, W. Chen, and J. Gao, “Improving Multi-Task Deep Neural Networks via Knowledge Distillation for Natural Language Understanding.” arXiv, Apr. 20, 2019. doi: 10.48550/arXiv.1904.09482.
[29] McMahon, “HESS - Comment on the application of the Szilagyi–Jozsa advection–aridity model for estimating actual terrestrial evapotranspiration in ‘Estimating actual, potential, reference crop and pan evaporation using standard meteorological data: a pragmatic synthesis’ by McMahon et al. (2013),” 2013. https://hess.copernicus.org/articles/17/4865/2013/ (accessed Nov. 29, 2022).
[30] P. Peng, T. Wang, C. Wang, and X. Lin, “A meta-analysis on the relation between fluid intelligence and reading/mathematics: Effects of tasks, age, and social economics status,” *Psychological Bulletin*, vol. 145, pp. 189–236, 2019, doi: 10.1037/bul0000182.
[31] S. Tasumi *et al.*, “A SNP in a Steroidogenic Enzyme Is Associated with Phenotypic Sex in Seriola Fishes,” *Current Biology*, vol. 29, no. 11, pp. 1901-1909.e8, Jun. 2019, doi: 10.1016/j.cub.2019.04.069.
[32] R. G. Allen, “Assessing Integrity of Weather Data for Reference Evapotranspiration Estimation,” *Journal of Irrigation and Drainage Engineering*, vol. 122, no. 2, pp. 97–106, Mar. 1996, doi: 10.1061/(ASCE)0733-9437(1996)122:2(97).
[33] S. Irmak and D. Z. Haman, “Evaluation of Five Methods for Estimating Class A Pan Evaporation in a Humid Climate,” *HortTechnology*, vol. 13, no. 3, pp. 500–508, Jan. 2003, doi: 10.21273/HORTTECH.13.3.0500.

[34] M. W. Peng, D. Ahlstrom, S. M. Carraher, and W. (Stone) Shi, “An institution-based view of global IPR history,” *J Int Bus Stud*, vol. 48, no. 7, pp. 893–907, Sep. 2017, doi: 10.1057/s41267-016-0061-9.
[35] D. Yates and K. M. Strzepek, “Potential Evapotranspiration Methods and their Impact on the Assessment of River Basin Runoff Under Climate Change,” Jul. 1994. https://iiasa.dev.local/ (accessed Nov. 29, 2022).
[36] J. Doorenbos, “Guidelines for predicting crop water requirements,” *Food and Agriculture organization. Rome, Irrig. Drainage pap.*, vol. 24, 1975, Accessed: Dec. 28, 2022. [Online]. Available: https://cir.nii.ac.jp/crid/1572824499960912768
[37] G. Hargreaves and Z. Samani, “Reference Crop Evapotranspiration From Temperature,” *Applied Engineering in Agriculture*, vol. 1, Jan. 1985, doi: 10.13031/2013.26773.
[38] Turc, “The water balance of soils. Relation between precipitation, evaporation and flow,” 1954.
[39] C. H. B. Priestley and R. J. Taylor, “On the Assessment of Surface Heat Flux and Evaporation Using Large-Scale Parameters,” *Monthly Weather Review*, vol. 100, no. 2, pp. 81–92, Feb. 1972, doi: 10.1175/1520-0493(1972)100<0081:OTAOSH>2.3.CO;2.
[40] M. I. Budyko, “The Heat Balance of the Earth’s Surface,” *Soviet Geography*, vol. 2, no. 4, pp. 3–13, Jan. 1961, doi: 10.1080/00385417.1961.10770761.
[41] L. Zhang, N. Potter, K. Hickel, Y. Zhang, and Q. Shao, “Water balance modeling over variable time scales based on the Budyko framework – Model development and testing,” *Journal of Hydrology*, vol. 360, no. 1, pp. 117–131, Oct. 2008, doi: 10.1016/j.jhydrol.2008.07.021.
[42] S. Traore and A. Guven, “Regional-Specific Numerical Models of Evapotranspiration Using Gene-Expression Programming Interface in Sahel,” *Water Resour Manage*, vol. 26, no. 15, pp. 4367–4380, Dec. 2012, doi: 10.1007/s11269-012-0149-3.
[43] X. Dou and Y. Yang, “Evapotranspiration estimation using four different machine learning approaches in different terrestrial ecosystems,” *Computers and Electronics in Agriculture*, vol. 148, pp. 95–106, May 2018, doi: 10.1016/j.compag.2018.03.010.
[44] L. B. Ferreira, F. F. da Cunha, R. A. de Oliveira, and E. I. Fernandes Filho, “Estimation of reference evapotranspiration in Brazil with limited meteorological data using ANN and SVM – A new approach,” *Journal of Hydrology*, vol. 572, pp. 556–570, May 2019, doi: 10.1016/j.jhydrol.2019.03.028.
[45] J. H. Friedman, “Greedy Function Approximation: A Gradient Boosting Machine,” *The Annals of Statistics*, vol. 29, no. 5, pp. 1189–1232, 2001.
[46] M. Kumar, N. S. Raghuwanshi, R. Singh, W. W. Wallender, and W. O. Pruitt, “Estimating Evapotranspiration using Artificial Neural Network,” *Journal of Irrigation and Drainage Engineering*, vol. 128, no. 4, pp. 224–233, Aug. 2002, doi: 10.1061/(ASCE)0733-9437(2002)128:4(224).
[47] M. Ehteram *et al.*, “An improved model based on the support vector machine and cuckoo algorithm for simulating reference evapotranspiration,” *PLOS ONE*, vol. 14, no. 5, p. e0217499, May 2019, doi: 10.1371/journal.pone.0217499.
[48] P. López López, E. H. Sutanudjaja, J. Schellekens, G. Sterk, and M. F. P. Bierkens, “Calibration of a large-scale hydrological model using satellite-based soil moisture and evapotranspiration products,” *Hydrology and Earth System*

Sciences, vol. 21, no. 6, pp. 3125–3144, Jun. 2017, doi: 10.5194/hess-21-3125-2017.
[49] L. Zhao, J. Xia, C. Xu, Z. Wang, L. Sobkowiak, and C. Long, “Evapotranspiration estimation methods in hydrological models,” *J. Geogr. Sci.*, vol. 23, no. 2, pp. 359–369, Apr. 2013, doi: 10.1007/s11442-013-1015-9.
[50] Q. Mu, M. Zhao, and S. Running, *Algorithm Theoretical Basis Document: MODIS Global Terrestrial Evapotranspiration (ET) Product (NASA MOD16A2/A3) Collection 5. NASA Headquarters*. 2013.
[51] M. Dorjsuren, Y.-A. Liou, and C.-H. Cheng, “Time Series MODIS and in Situ Data Analysis for Mongolia Drought,” *Remote Sensing*, vol. 8, no. 6, Art. no. 6, Jun. 2016, doi: 10.3390/rs8060509.
[52] K. Szewczak *et al.*, “Agricultural Drought Monitoring by MODIS Potential Evapotranspiration Remote Sensing Data Application,” *Remote Sensing*, vol. 12, no. 20, Art. no. 20, Jan. 2020, doi: 10.3390/rs12203411.
[53] J. Baik, U. W. Liaqat, and M. Choi, “Assessment of satellite- and reanalysis-based evapotranspiration products with two blending approaches over the complex landscapes and climates of Australia,” *Agricultural and Forest Meteorology*, vol. 263, pp. 388–398, Dec. 2018, doi: 10.1016/j.agrformet.2018.09.007.
[54] J. Kim and T. S. Hogue, “Evaluation of a MODIS-Based Potential Evapotranspiration Product at the Point Scale,” *Journal of Hydrometeorology*, vol. 9, no. 3, pp. 444–460, Jun. 2008, doi: 10.1175/2007JHM902.1.
[55] O. O. Ayantobo and J. Wei, “Appraising regional multi-category and multi-scalar drought monitoring using standardized moisture anomaly index (SZI): A water-energy balance approach,” *Journal of Hydrology*, vol. 579, p. 124139, Dec. 2019, doi: 10.1016/j.jhydrol.2019.124139.
[56] S. Rehana, P. P. Mujumdar, and R. Meenu, “Assessment of hydrologic impacts of climate change in Tunga–Bhadra river basin, India with HEC-HMS and SDSM,” *Hydrological Processes*, vol. 27, no. 11, pp. 1572–1589, 2013, doi: 10.1002/hyp.9220.
[57] P. P. Mujumdar and S. Ghosh, “Modeling GCM and scenario uncertainty using a possibilistic approach: Application to the Mahanadi River, India,” *Water Resources Research*, vol. 44, no. 6, 2008, doi: 10.1029/2007WR006137.
[58] W. S. McCulloch and W. Pitts, “A logical calculus of the ideas immanent in nervous activity,” *Bulletin of Mathematical Biophysics*, vol. 5, no. 4, pp. 115–133, Dec. 1943, doi: 10.1007/BF02478259.
[59] K. W. Daniel, N. K. Tripathi, and K. Honda, “Artificial neural network analysis of laboratory and in situ spectra for the estimation of macronutrients in soils of Lop Buri (Thailand),” *Soil Res.*, vol. 41, no. 1, pp. 47–59, 2003, doi: 10.1071/sr02027.
[60] A. Dikshit, B. Pradhan, and A. M. Alamri, “Short-Term Spatio-Temporal Drought Forecasting Using Random Forests Model at New South Wales, Australia,” *Applied Sciences*, vol. 10, no. 12, Art. no. 12, Jan. 2020, doi: 10.3390/app10124254.
[61] B. Ming, Y. Guo, H. Tao, G. Liu, S. Li, and P. Wang, “SPEIPM-based research on drought impact on maize yield in North China Plain,” *Journal of Integrative Agriculture*, vol. 14, no. 4, pp. 660–669, Apr. 2015, doi: 10.1016/S2095-3119(14)60778-4.
[62] S. K. Jain, P. C. Nayak, and K. P. Sudheer, “Models for estimating evapotranspiration using artificial neural networks, and their physical

interpretation," *Hydrological Processes*, vol. 22, no. 13, pp. 2225–2234, 2008, doi: 10.1002/hyp.6819.

[63] Fu, B.P., "Fu, B.P. (1981) On the Calculation of the Evaporation from Land Surface. Scientia Atmospherica Sinica, 5, 23-31. - References - Scientific Research Publishing," 1981. https://www.scirp.org/%28S%28vtj3fa45qm1ean45vvffcz55%29%29/reference/referencespapers.aspx?referenceid=1185500 (accessed Apr. 23, 2022).

[64] J. B. Schreiber, A. Nora, F. K. Stage, E. A. Barlow, and J. King, "Reporting Structural Equation Modeling and Confirmatory Factor Analysis Results: A Review," *The Journal of Educational Research*, vol. 99, no. 6, pp. 323–338, Jul. 2006, doi: 10.3200/JOER.99.6.323-338.

[65] M. K. Goyal, B. Bharti, J. Quilty, J. Adamowski, and A. Pandey, "Modeling of daily pan evaporation in sub tropical climates using ANN, LS-SVR, Fuzzy Logic, and ANFIS," *Expert Systems with Applications*, vol. 41, no. 11, pp. 5267–5276, Sep. 2014, doi: 10.1016/j.eswa.2014.02.047.

[66] K. Abbaspour, S. A. Naghibi, and H. R. Pourghasemi, "A comparison between ten advanced and soft computing models for groundwater qanat potential assessment in Iran using R and GIS," *Theor Appl Climatol*, vol. 131, no. 3, pp. 967–984, Feb. 2018, doi: 10.1007/s00704-016-2022-4.

[67] Mallya, "Trends and variability of droughts over the Indian monsoon region - ScienceDirect," 2016. https://www.sciencedirect.com/science/article/pii/S2212094715300578 (accessed Dec. 24, 2022).

[68] S. Rehana and N. T. Monish, "Characterization of Regional Drought Over Water and Energy Limited Zones of India Using Potential and Actual Evapotranspiration," *Earth and Space Science*, vol. 7, no. 10, p. e2020EA001264, 2020, doi: 10.1029/2020EA001264.

[69] F. A. M. Al-Faraj, M. Scholz, and D. Tigkas, "Sensitivity of Surface Runoff to Drought and Climate Change: Application for Shared River Basins," *Water*, vol. 6, no. 10, Art. no. 10, Oct. 2014, doi: 10.3390/w6103033.